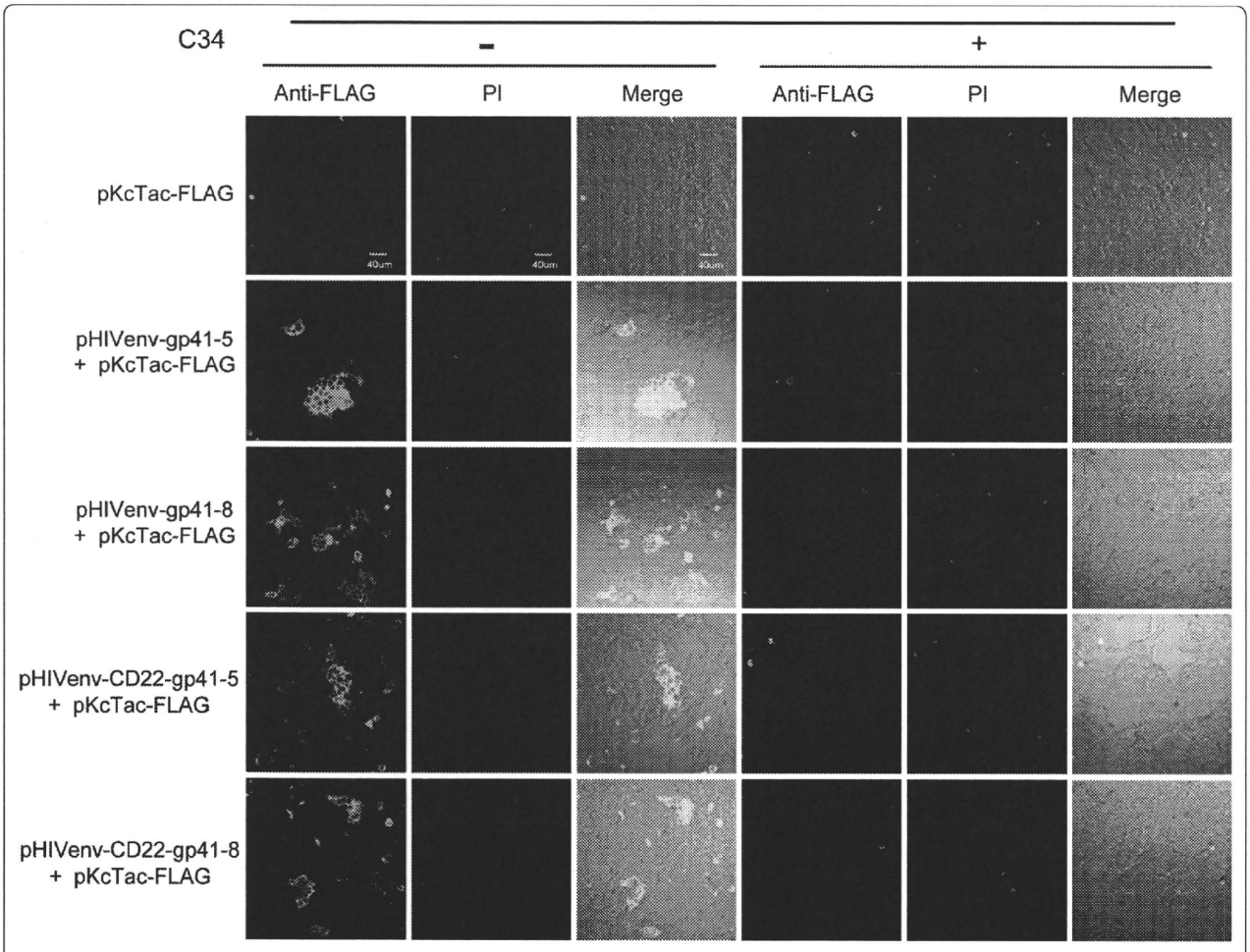

Figure 8 Examination of membrane permeability during membrane fusion using antibodies as probes. Staining of 293CD4 cells cotransfected with the Env expression vector and pKcTac-FLAG in the presence (+) or absence (-) of C34 by anti-FLAG antibody. The pKcTac-FLAG vector expresses the Tac proteins tagged with FLAG at their C-termini. Anti-FLAG: images after staining with the anti-FLAG antibody as described in Methods are shown in green. The time points for the assay were same as Fig. 7 (16 h post transfection for wild type MSDs and 44 h for CD22MSDs, respectively). PI: Images after propidium iodide staining. Merge: merged images of Anti-FLAG and PI stainings together with that of bright fields. The concentration of C34 was 2 μM. The names of the expression vectors used are shown in left. The bar indicates 40 μm.

It is known that the several isolated subdomains of gp41, critical for membrane fusion, have potential to permeabilize the mammalian and the bacterial membranes [39-50]. These include the fusion peptide, the membrane proximate external region, the MSD and the LLPs. Our data of pHIVenv-gp41-5 (Figure 7 and 8) excludes the possibility of the role of LLPs. Our data using MSD replacement mutants pHIVenv-CD22-gp41-5 or pHIVenv-CD22-gp41-8, suggested the MSD affected the level of permeability, but whether the MSD directly affected the permeability or the effect was mediated via the efficiency of the membrane fusion was hard to be determined.

Since our assay relied on the topological reporter proteins attached at the C-termini of truncated gp41 proteins, the possibility of artifacts cannot be excluded. The exact reason why neutralizing epitopes mapped to the cytoplasmic regions remains unclear. There are at least two possible explanations. First, it is possible that the some of the antibodies themselves are intrinsically membrane permeable. Second, permeability that is sufficient to permit antibodies to cross the membrane may be induced by membrane fusion. Although our findings support the latter model, further study is needed to explore whether an alternative topology for gp41 MSD during membrane fusion really takes place and if such a possibility is a general phenomenon for other HIV-1 strains.

Conclusions

The membrane topology of the gp41 subunit of HIV-1 Env was examined in both prokaryotic and mammalian systems. The topology with a single MSD was supported in both systems. In addition, augmented membrane

permeability was shown to be dependent on both the sequence of MSD and active membrane fusion.

List of abbreviations

Env: envelope glycoprotein; HIV-1: human immunodeficiency virus type-1; LLP: lentiviral lytic peptide; MSD: membrane-spanning domain; GFP: green fluorescent protein; GPI: glycosylphosphatidylinositol; FBS: fetal bovine serum; OG: Oregon Green; AF488: Alexa Fluor 488; PI: propidium iodide; PBS: phosphate buffered saline.

Acknowledgements

This work was supported by a contract research fund from the Ministry of Education, Culture, Sports, Science and Technology for Program of Japan Initiative for Global Research Network on Infectious Diseases. We thank Dr. Kunito Yoshiike for his critical reading of the manuscript.

Additional material

Additional file 1: Supplemental Fig.1 Detection of HaloTag-attached HIV-1 Env in 293FT cells. Images of the transfected 293FT cells stained with membrane-permeable ligand, Oregon Green (OG). BF indicates the bright filed images. The names of the expression vectors are shown. Mock, mock DNA transfection.

Additional file 2: Supplemental Fig.2 Detection of HaloTag-attached HIV-1 Env in 293CD4 cells. Images of the transfected 293CD4 cells stained with membrane permeable ligand, Oregon Green (OG). The nomenclature used are same as Supple Figure 1.

Additional file 3: Supplemental Fig.3 Expression of HIV-1 Env with its native MSD or foreign CD22MSD in 293FT cells. The expression of the envelope protein was examined by immunoblotting using the anti-gp120 antibody as described previously [23]. The names of the expression vectors were shown on top. The bands of gp160 and gp120 are indicated.

Author details

[1]China-Japan Joint Laboratory of Structural Virology and Immunology, Institute of Biophysics, Chinese Academy of Sciences, 15 Datun Road, Chaoyang District, Beijing 100101, P. R. China. [2]Research Center for Asian Infectious Diseases, and 3Division of Infectious Diseases, Advanced Clinical Research Center, Institute of Medical Science, University of Tokyo, 4-6-1, Shirokanedai Minato-ku, Tokyo 108-8639, Japan. [3]Current Address: Department of Pediatrics, Emory University School of Medicine, 2015 uppergate Dr. Atlanta, GA 30322, USA.

Authors' contributions

SL, NK, YL and DX performed the experiments. The analysis in the prokaryotic system was done by SL and DX. The work in mammalian system was performed by SL, NK and YL. The study was conceived by ZM. AI supervised the entire work. SL, NK and ZM wrote the manuscript. All authors read and approved the final manuscript.

Competing interests

The authors declare that they have no competing interests.

Received: 13 July 2010 Accepted: 30 November 2010
Published: 30 November 2010

References

1. Dettenhofer M, Yu XF: **Characterization of the biosynthesis of human immunodeficiency virus type 1 Env from infected T-cells and the effects of glucose trimming of Env on virion infectivity.** *J Biol Chem* 2001, **276**:5985-5991.
2. Otteken A, Earl PL, Moss B: **Folding, assembly, and intracellular trafficking of the human immunodeficiency virus type 1 envelope glycoprotein analyzed with monoclonal antibodies recognizing maturational intermediates.** *J Virol* 1996, **70**:3407-3415.
3. Dash B, McIntosh A, Barrett W, Daniels R: **Deletion of a single N-linked glycosylation site from the transmembrane envelope protein of human immunodeficiency virus type 1 stops cleavage and transport of gp160 preventing env-mediated fusion.** *J Gen Virol* 1994, **75(Pt 6)**:1389-1397.
4. Fenouillet E, Jones IM: **The glycosylation of human immunodeficiency virus type 1 transmembrane glycoprotein (gp41) is important for the efficient intracellular transport of the envelope precursor gp160.** *J Gen Virol* 1995, **76(Pt 6)**:1509-1514.
5. Eisenberg D, Wesson M: **The most highly amphiphilic alpha-helices include two amino acid segments in human immunodeficiency virus glycoprotein 41.** *Biopolymers* 1990, **29**:171-177.
6. Kliger Y, Shai Y: **A leucine zipper-like sequence from the cytoplasmic tail of the HIV-1 envelope glycoprotein binds and perturbs lipid bilayers.** *Biochemistry* 1997, **36**:5157-5169.
7. Gawrisch K, Han KH, Yang JS, Bergelson LD, Ferretti JA: **Interaction of peptide fragment 828-848 of the envelope glycoprotein of human immunodeficiency virus type I with lipid bilayers.** *Biochemistry* 1993, **32**:3112-3118.
8. Srinivas SK, Srinivas RV, Anantharamaiah GM, Segrest JP, Compans RW: **Membrane interactions of synthetic peptides corresponding to amphipathic helical segments of the human immunodeficiency virus type-1 envelope glycoprotein.** *J Biol Chem* 1992, **267**:7121-7127.
9. Viard M, Ablan SD, Zhou M, Veenstra TD, Freed EO, Raviv Y, Blumenthal R: **Photoinduced reactivity of the HIV-1 envelope glycoprotein with a membrane-embedded probe reveals insertion of portions of the HIV-1 Gp41 cytoplasmic tail into the viral membrane.** *Biochemistry* 2008, **47**:1977-1983.
10. Muesing MA, Smith DH, Cabradilla CD, Benton CV, Lasky LA, Capon DJ: **Nucleic acid structure and expression of the human AIDS/lymphadenopathy retrovirus.** *Nature* 1985, **313**:450-458.
11. Haffar OK, Dowbenko DJ, Berman PW: **Topogenic analysis of the human immunodeficiency virus type 1 envelope glycoprotein, gp160, in microsomal membranes.** *J Cell Biol* 1988, **107**:1677-1687.
12. Yang C, Spies CP, Compans RW: **The human and simian immunodeficiency virus envelope glycoprotein transmembrane subunits are palmitoylated.** *Proc Natl Acad Sci USA* 1995, **92**:9871-9875.
13. Rowell JF, Stanhope PE, Siliciano RF: **Endocytosis of endogenously synthesized HIV-1 envelope protein. Mechanism and role in processing for association with class II MHC.** *J Immunol* 1995, **155**:473-488.
14. Kennedy RC, Henkel RD, Pauletti D, Allan JS, Lee TH, Essex M, Dreesman GR: **Antiserum to a synthetic peptide recognizes the HTLV-III envelope glycoprotein.** *Science* 1986, **231**:1556-1559.
15. Vella C, Ferguson M, Dunn G, Meloen R, Langedijk H, Evans D, Minor PD: **Characterization and primary structure of a human immunodeficiency virus type 1 (HIV-1) neutralization domain as presented by a poliovirus type 1/HIV-1 chimera.** *J Gen Virol* 1993, **74(Pt 12)**:2603-2607.
16. Cleveland SM, McLain L, Cheung L, Jones TD, Hollier M, Dimmock NJ: **A region of the C-terminal tail of the gp41 envelope glycoprotein of human immunodeficiency virus type 1 contains a neutralizing epitope: evidence for its exposure on the surface of the virion.** *J Gen Virol* 2003, **84**:591-602.
17. Lu L, Zhu Y, Huang J, Chen X, Yang H, Jiang S, Chen YH: **Surface exposure of the HIV-1 env cytoplasmic tail LLP2 domain during the membrane fusion process: interaction with gp41 fusion core.** *J Biol Chem* 2008, **283**:16723-16731.
18. Yue L, Shang L, Hunter E: **Truncation of the membrane-spanning domain of human immunodeficiency virus type 1 envelope glycoprotein defines elements required for fusion, incorporation, and infectivity.** *J Virol* 2009, **83**:11588-11598.
19. Shang L, Yue L, Hunter E: **Role of the membrane-spanning domain of human immunodeficiency virus type 1 envelope glycoprotein in cell-cell fusion and virus infection.** *J Virol* 2008, **82**:5417-5428.
20. Salzwedel K, Johnston PB, Roberts SJ, Dubay JW, Hunter E: **Expression and characterization of glycophospholipid-anchored human immunodeficiency virus type 1 envelope glycoproteins.** *J Virol* 1993, **67**:5279-5288.
21. Weiss CD, White JM: **Characterization of stable Chinese hamster ovary cells expressing wild-type, secreted, and glycosylphosphatidylinositol-**

anchored human immunodeficiency virus type 1 envelope glycoprotein. *J Virol* 1993, **67**:7060-7066.

22. Owens RJ, Burke C, Rose JK: **Mutations in the membrane-spanning domain of the human immunodeficiency virus envelope glycoprotein that affect fusion activity.** *J Virol* 1994, **68**:570-574.
23. Miyauchi K, Komano J, Yokomaku Y, Sugiura W, Yamamoto N, Matsuda Z: **Role of the specific amino acid sequence of the membrane-spanning domain of human immunodeficiency virus type 1 in membrane fusion.** *J Virol* 2005, **79**:4720-4729.
24. Miyauchi K, Curran R, Matthews E, Komano J, Hoshino T, Engelman DM, Matsuda Z: **Mutations of conserved glycine residues within the membrane-spanning domain of human immunodeficiency virus type 1 gp41 can inhibit membrane fusion and incorporation of Env onto virions.** *Jpn J Infect Dis* 2006, **59**:77-84.
25. Wang J, Kondo N, Long Y, Iwamoto A, Matsuda Z: **Monitoring of HIV-1 envelope-mediated membrane fusion using modified split green fluorescent proteins.** *J Virol Methods* 2009, **161**:216-222.
26. Kondo N, Ebihara A, Ru H, Kuramitsu S, Iwamoto A, Rao Z, Matsuda Z: **Thermus thermophilus-derived protein tags that aid in preparation of insoluble viral proteins.** *Anal Biochem* 2009, **385**:278-285.
27. Wilk T, Pfeiffer T, Bukovsky A, Moldenhauer G, Bosch V: **Glycoprotein incorporation and HIV-1 infectivity despite exchange of the gp160 membrane-spanning domain.** *Virology* 1996, **218**:269-274.
28. Caras IW, Weddell GN, Williams SR: **Analysis of the signal for attachment of a glycophospholipid membrane anchor.** *J Cell Biol* 1989, **108**:1387-1396.
29. Cosson P, Lankford SP, Bonifacino JS, Klausner RD: **Membrane protein association by potential intramembrane charge pairs.** *Nature* 1991, **351**:414-416.
30. van Genderen H, Kenis H, Lux P, Ungeth L, Maassen C, Deckers N, Narula J, Hofstra L, Reutelingsperger C: **In vitro measurement of cell death with the annexin A5 affinity assay.** *Nat Protoc* 2006, **1**:363-367.
31. Drew D, Sjostrand D, Nilsson J, Urbig T, Chin CN, de Gier JW, von Heijne G: **Rapid topology mapping of Escherichia coli inner-membrane proteins by prediction and PhoA/GFP fusion analysis.** *Proc Natl Acad Sci USA* 2002, **99**:2690-2695.
32. Duffy EB, Barquera B: **Membrane topology mapping of the Na+-pumping NADH: quinone oxidoreductase from Vibrio cholerae by PhoA-green fluorescent protein fusion analysis.** *J Bacteriol* 2006, **188**:8343-8351.
33. Los GV, Encell LP, McDougall MG, Hartzell DD, Karassina N, Zimprich C, Wood MG, Learish R, Ohana RF, Urh M, *et al*: **HaloTag: a novel protein labeling technology for cell imaging and protein analysis.** *ACS Chem Biol* 2008, **3**:373-382.
34. Kondo N, Miyauchi K, Meng F, Iwamoto A, Matsuda Z: **Conformational changes of the HIV-1 envelope protein during membrane fusion are inhibited by the replacement of its membrane-spanning domain.** *J Biol Chem* 2010, **285**:14681-14688.
35. Cloyd MW, Lynn WS: **Perturbation of host-cell membrane is a primary mechanism of HIV cytopathology.** *Virology* 1991, **181**:500-511.
36. Zhang H, Dornadula G, Alur P, Laughlin MA, Pomerantz RJ: **Amphipathic domains in the C terminus of the transmembrane protein (gp41) permeabilize HIV-1 virions: a molecular mechanism underlying natural endogenous reverse transcription.** *Proc Natl Acad Sci USA* 1996, **93**:12519-12524.
37. Gatti PJ, Choi B, Haislip AM, Fermin CD, Garry RF: **Inhibition of HIV type 1 production by hygromycin B.** *AIDS Res Hum Retroviruses* 1998, **14**:885-892.
38. Voss TG, Fermin CD, Levy JA, Vigh S, Choi B, Garry RF: **Alteration of intracellular potassium and sodium concentrations correlates with induction of cytopathic effects by human immunodeficiency virus.** *J Virol* 1996, **70**:5447-5454.
39. Miller MA, Cloyd MW, Liebmann J, Rinaldo CR, Islam KR, Wang SZ, Mietzner TA, Montelaro RC: **Alterations in cell membrane permeability by the lentivirus lytic peptide (LLP-1) of HIV-1 transmembrane protein.** *Virology* 1993, **196**:89-100.
40. Chernomordik L, Chanturiya AN, Suss-Toby E, Nora E, Zimmerberg J: **An amphipathic peptide from the C-terminal region of the human immunodeficiency virus envelope glycoprotein causes pore formation in membranes.** *J Virol* 1994, **68**:7115-7123.
41. Arroyo J, Boceta M, Gonzalez ME, Michel M, Carrasco L: **Membrane permeabilization by different regions of the human immunodeficiency virus type 1 transmembrane glycoprotein gp41.** *J Virol* 1995, **69**:4095-4102.
42. Comardelle AM, Norris CH, Plymale DR, Gatti PJ, Choi B, Fermin CD, Haislip AM, Tencza SB, Mietzner TA, Montelaro RC, Garry RF: **A synthetic peptide corresponding to the carboxy terminus of human immunodeficiency virus type 1 transmembrane glycoprotein induces alterations in the ionic permeability of Xenopus laevis oocytes.** *AIDS Res Hum Retroviruses* 1997, **13**:1525-1532.
43. Suarez T, Gallaher WR, Agirre A, Goni FM, Nieva JL: **Membrane interface-interacting sequences within the ectodomain of the human immunodeficiency virus type 1 envelope glycoprotein: putative role during viral fusion.** *J Virol* 2000, **74**:8038-8047.
44. Suarez T, Nir S, Goni FM, Saez-Cirion A, Nieva JL: **The pre-transmembrane region of the human immunodeficiency virus type-1 glycoprotein: a novel fusogenic sequence.** *FEBS Lett* 2000, **477**:145-149.
45. Brugger B, Glass B, Haberkant P, Leibrecht I, Wieland FT, Krausslich HG: **The HIV lipidome: a raft with an unusual composition.** *Proc Natl Acad Sci USA* 2006, **103**:2641-2646.
46. Saez-Cirion A, Arrondo JL, Gomara MJ, Lorizate M, Iloro I, Melikyan G, Nieva JL: **Structural and functional roles of HIV-1 gp41 pretransmembrane sequence segmentation.** *Biophys J* 2003, **85**:3769-3780.
47. Saez-Cirion A, Nir S, Lorizate M, Agirre A, Cruz A, Perez-Gil J, Nieva JL: **Sphingomyelin and cholesterol promote HIV-1 gp41 pretransmembrane sequence surface aggregation and membrane restructuring.** *J Biol Chem* 2002, **277**:21776-21785.
48. Apellaniz B, Nir S, Nieva JL: **Distinct mechanisms of lipid bilayer perturbation induced by peptides derived from the membrane-proximal external region of HIV-1 gp41.** *Biochemistry* 2009, **48**:5320-5331.
49. Huarte N, Lorizate M, Kunert R, Nieva JL: **Lipid modulation of membrane-bound epitope recognition and blocking by HIV-1 neutralizing antibodies.** *FEBS Lett* 2008, **582**:3798-3804.
50. Dimitrov AS, Rawat SS, Jiang S, Blumenthal R: **Role of the fusion peptide and membrane-proximal domain in HIV-1 envelope glycoprotein-mediated membrane fusion.** *Biochemistry* 2003, **42**:14150-14158.

doi:10.1186/1742-4690-7-100
Cite this article as: Liu *et al.*: Membrane topology analysis of HIV-1 envelope glycoprotein gp41. *Retrovirology* 2010 **7**:100.

622 J. Med. Chem. 2011, 54, 622–634
DOI: 10.1021/jm1012787

Journal of Medicinal Chemistry Article

Design and Synthesis of Potent HIV-1 Protease Inhibitors Incorporating Hexahydrofuropyranol-Derived High Affinity P_2 Ligands: Structure−Activity Studies and Biological Evaluation

Arun K. Ghosh,*[,†,‡] Bruno D. Chapsal,[†] Abigail Baldridge,[†] Melinda P. Steffey,[†] D. Eric Walters,[§] Yasuhiro Koh,[∥,⊥] Masayuki Amano,[∥,⊥] and Hiroaki Mitsuya[∥,⊥,#]

[†]*Department of Chemistry, and* [‡]*Department of Medicinal Chemistry, Purdue University, West Lafayette, Indiana 47907, United States,* [§]*Department of Biochemistry and Molecular Biology, Rosalind Franklin University of Medicine and Science, North Chicago, Illinois 60064, United States,* [∥]*Department of Hematology, and* [⊥]*Department of Infectious Diseases, Kumamoto University School of Medicine, Kumamoto 860-8556, Japan, and* [#]*Experimental Retrovirology Section, HIV and AIDS Malignancy Branch, National Cancer Institute, Bethesda, Maryland 20892, United States*

Received October 4, 2010

The design, synthesis, and evaluation of a new series of hexahydrofuropyranol-derived HIV-1 protease inhibitors are described. We have designed a stereochemically defined hexahydrofuropyranol-derived urethane as the P2-ligand. The current ligand is designed based upon the X-ray structure of **1a**-bound HIV-1 protease. The synthesis of (3a*S*,4*S*,7a*R*)-hexahydro-2*H*-furo[2,3-*b*]pyran-4-ol, (−)-**7**, was carried out in optically active form. Incorporation of this ligand provided inhibitor **35a**, which has shown excellent enzyme inhibitory activity and antiviral potency. Our structure−activity studies have indicated that the stereochemistry and the position of oxygens in the ligand are important to the observed potency of the inhibitor. Inhibitor **35a** has maintained excellent potency against multidrug-resistant HIV-1 variants. An active site model of **35a** was created based upon the X-ray structure of **1b**-bound HIV-1 protease. The model offers molecular insights regarding ligand-binding site interactions of the hexahydrofuropyranol-derived novel P2-ligand.

Introduction

HIV-1 protease inhibitors are critical components of highly active antiretroviral therapy (HAART[a]).[1−3] The HAART treatment regimens significantly reduced HIV/AIDS-related mortality.[4,5] However, the rapid emergence of drug-resistant HIV-1 strains and the appearance of cross-resistance are severely limiting long-term treatment options.[6−8] An estimated 10−25% of newly infected patients harbor at least one viral strain that is resistant to current medications.[9−11] In addition, PI regimens suffer from a number of other drawbacks including high pill burden, treatment cost, poor ADMET properties, debilitating side effects, and toxicity issues.[12] Therefore, the development of novel PIs with broad-spectrum activity against multidrug-resistant HIV-1 variants remains a major therapeutic objective.[13]

In our continuing interest to develop novel protease inhibitors (PI) with broad-spectrum activity against multidrug-resistant HIV-1 variants, we have reported a series of PIs including PIs **1a**, **1b**, **2**, and **3**.[14−16] These inhibitors exhibited excellent antiviral activity against multidrug-resistant HIV-1 variants. Darunavir (TMC-114, Figure 1) has been recently approved by the FDA.[17,18] It has displayed a high genetic barrier to resistance and retained high potency against multidrug resistant HIV-1 strains. It has been demonstrated that resistance to **1a** is significantly delayed compared to other approved PIs.[19−21]

Our structure-based design of **1a** and other PIs is inspired by the premise that an inhibitor engaged in multiple interactions, especially hydrogen bonding with the HIV protease backbone atoms, should retain these affinities with mutant strains.[22] As the enzyme backbone conformation is only minimally distorted when mutations occur, backbone atoms−PI interactions are likely maintained, therefore sustaining the inhibitor affinity and potency. Inhibitor **1a**'s superb resistance profile likely originates from the extensive interactions the inhibitor makes within the HIV-1 protease's binding site and particularly with the backbone atoms of the enzyme.[22−24] Extensive studies of **1a**-bound HIV-1 protease crystal structures have consistently revealed tight hydrogen bonding between the inhibitor and the protease backbone.[23−25] The stereochemically defined bis-tetrahydrofuran (bis-THF) P_2 ligand in **1a** forms a strong hydrogen bonding network between its two cyclic ether oxygens and the backbone amide NH bonds of the protease residues, Asp29 and Asp30.[22] These observations likely provide explanations for **1a**'s outstanding antiviral activity. Not surprisingly, several other protease inhibitors featuring the bis-THF as the P_2 ligand have exhibited equally impressive antiviral activities and resistance profiles.[22,26]

The bis-THF ligand represents an intriguing pharmacophoric scaffold for the development of PIs to combat drug resistance. To further optimize the bis-THF structural template, we have now investigated ligands that could enhance the backbone-binding as well as improve hydrophobic interactions with the protease active site. The X-ray structure of **1a**-bound HIV-1 protease has shown a distance of about 3.0−3.2 Å

*To whom correspondence should be addressed. Phone: (765)-494-5323. Fax: (765)-496-1612. E-mail: akghosh@purdue.edu.

[a] Abbreviations: bis-THF, bis-tetrahydrofuran; Cp-THF, cyclopentanyltetrahydrofuran; Tp-THF, tetrahydropyranyltetrahydrofuran; PI, protease inhibitor; HAART, highly active antiretroviral therapy; APV, amprenavir; DRV, darunavir; SQV, saquinavir; IDV, indinavir; LPV, lopinavir; RTV, ritonavir; ATV, atazanavir.

 Published on Web 12/31/2010

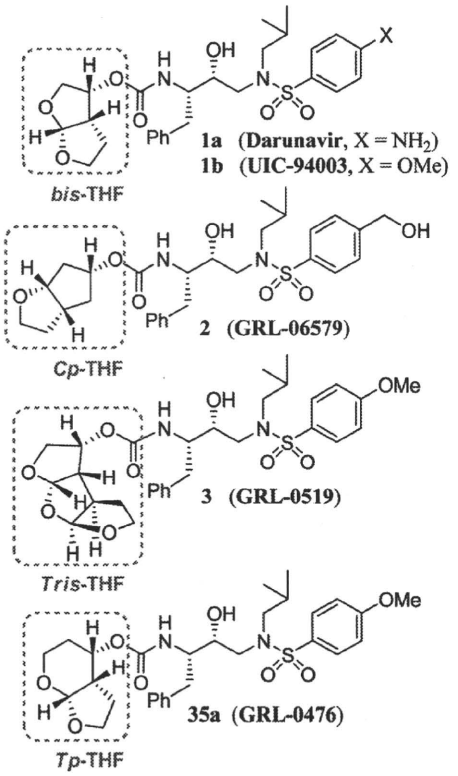

Figure 1. Structures of inhibitors **1**–**3** and **35a**.

between the bis-THF cyclic oxygens and the Asp30 NH amide bond, while a shorter 2.9 Å distance was observed with the Asp29 NH bond.[23,25] In order to maximize and promote closer hydrogen bonding with the Asp30 backbone NH bond, we thought a larger ring on the P_2 ligand should increase the dihedral angle of the bicyclic acetal, bring the oxygen closer, give more flexibility to the structure, and offer a more optimal alignment of the cyclic oxygen with the Asp30 NH bond. Such factors could realistically promote tighter hydrogen bonding with the Asp30 backbone NH bond. Besides, this extra methylene group in the "inner" ring would also provide more favorable van der Waals interactions within the hydrophobic pocket created by Ile47, Val32, Ile84, Leu76, and Ile50′ residues in the protease S_2 subsite. In addition, a larger ring could potentially lead to better flexibility and adaptability to protease mutations. Herein, we report the design, synthesis, and biological evaluation of a series of highly potent PIs that combined a (*R*)-hydroxyethylsulfonamide isostere with the furopyranol ligand (−)-**7**. Among all inhibitors of the series, **35a** showed the most impressive inhibitory and antiviral activity (K_i = 2.7 pM, IC_{50} = 0.5 nM). Moreover, inhibitor **35a** was evaluated against a panel of multidrug-resistant HIV-1 viruses. It retained potent activity against a variety of multidrug-resistant clinical HIV-1 strains with EC_{50} values in low nanomolar range, which is superior to other PIs and comparable to **1a**. Modeling of **35a** based upon the X-ray structure of **1b**-bound HIV-1 protease active site has provided critical molecular insight into the ligand-binding site interactions.

Chemistry

The synthesis of enantiomerically pure (3a*S*,4*S*,7a*R*)-hexahydro-2*H*-furo[2,3-*b*]pyran-4-ol is shown in Scheme 1. It was achieved starting from known enantiomerically pure lactone **4**.[27] Lactone **4** was reduced into the corresponding

Scheme 1. Synthesis of Ligand (−)-**7** and Its Respective Enantiomer (+)-**7**

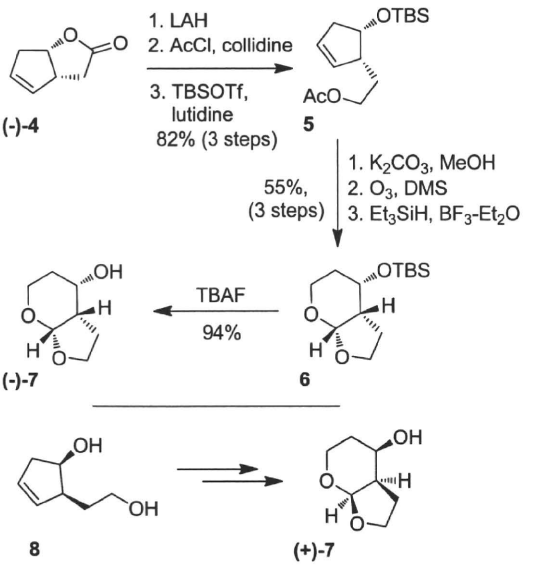

diol using lithium aluminum hydride in 95% yield. Selective monoacetylation at the primary alcohol using AcCl and 2,4,6-collidine at −78 °C[28] and subsequent silylation of the remaining free hydroxyl furnished intermediate **5** in 86% yield (two steps). Removal of the acetate group, followed by ozonolysis of the olefin, furnished a bicyclic bis-acetal intermediate. Reduction of the hemiacetal moiety using Et_3SiH and BF_3−Et_2O afforded bicyclic intermediate **6** in 55% yield in three steps. Removal of the silyl group with TBAF in THF furnished the desired hexahydrofuropyran-4-ol ligand (−)-**7**.

To demonstrate the importance of the absolute stereochemistry of the bicyclic structure of ligand (−)-**7**, its corresponding enantiomer (+)-**7** was synthesized starting from intermediate **8** (Scheme 1). Intermediate **8** was synthesized by an enzyme-catalyzed desymmetrization of cyclopentene *meso*-diacetate followed by a Claisen rearrangement step.[27b,29] The resulting diester was reduced by LAH to provide **8**. It was used for the synthesis of (+)-**7** and subjected to the same synthetic sequence applied from lactone (−)-**4** in the synthesis of (−)-**7** (Scheme 1). To examine the importance of each of the two cyclic ether oxygens in the furopyranol ligand (−)-**7**, we prepared the corresponding cyclohexane and cyclopentane derivatives (Schemes 2 and 3).

The synthesis of 4-hydroxyoctahydrobenzofuran ligand (−)-**12** is shown in Scheme 2. Reaction of diazocyclohexanedione **9**[30] with ethyl vinyl ether in presence of a catalytic amount of $Rh_2(OAc)_4$ at 23 °C gave derivative **10**.[31] Hydrogenation of the ketofuran in the presence of Pd/C under H_2 (1 atm) furnished the corresponding crude ketone **11** as a 9:1 mixture of diastereoisomers. A one-pot procedure involving L-selectride reduction of the ketone followed by Et_3SiH/TMSOTf-promoted reduction of the acetal furnished the racemic alcohol (±)-**12** (71% from **10**). Enzymatic resolution of (±)-**12** using lipase Amano PS-30 provided the desired enantiopure alcohol (−)-**12** (98.8% ee by chiral HPLC analysis of the 2,4-dinitrobenzoate derivative), after ~55% conversion to the acetate.

The synthesis of cyclopentapyranol ligand (−)-**18** is shown in Scheme 3. Pentanone **14** was treated with LDA and then reacted with *tert*-butyldimethylsilyloxypropionaldehyde[32]

Scheme 2. Synthesis of Furocyclohexanol P_2 Ligand (−)-**12**

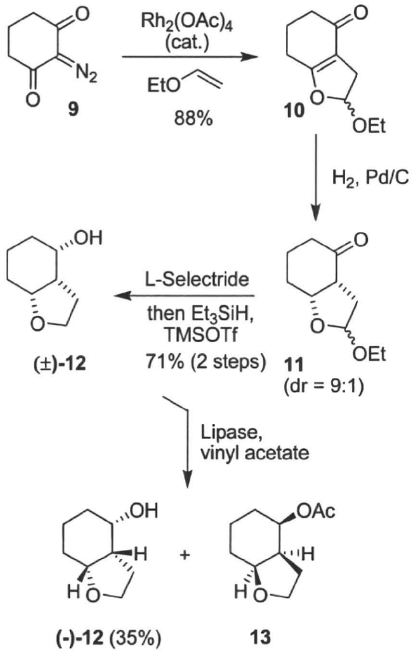

Scheme 3. Syntheses of Ligands (−)-**18** and (−)-**19**

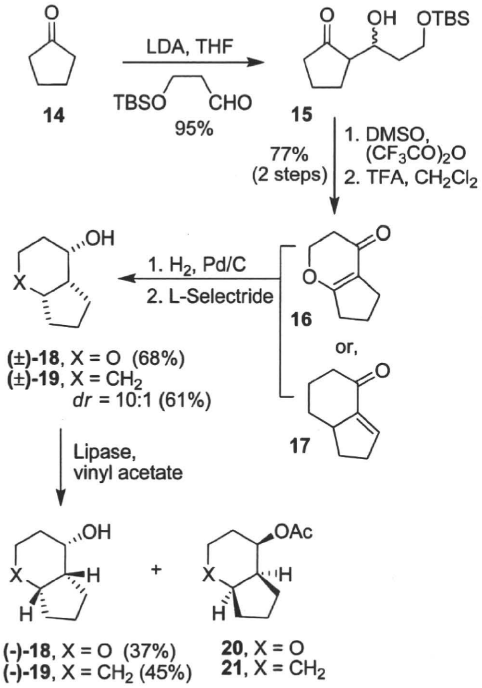

to furnish intermediate **15** (dr 3:1) in 95% yield. A DMSO-TFAA promoted oxidation of the free hydroxy group followed by TFA-promoted cyclocondensation furnished the bicyclic α,β-unsaturated ketone **16**. Hydrogenation in presence of 10% Pd/C followed by L-selectride reduction of the ketone gave racemic alcohol (±)-**18** as a single diastereomer in 68% yield over two steps. Lipase-catalyzed resolution of the alcohol provided enantiomerically pure alcohol (−)-**18**. For the synthesis of a P2 ligand devoid of any cyclic oxygen, known tetrahydroindanone **17**[33] was similarly hydrogenated in presence of 10% Pd/C to give the corresponding bicyclic ketone. Accordingly, L-selectride-promoted reduction of the

Scheme 4. Synthesis of Hexahydrofuro[3,4-*b*]pyran-4-ol Ligand **25**

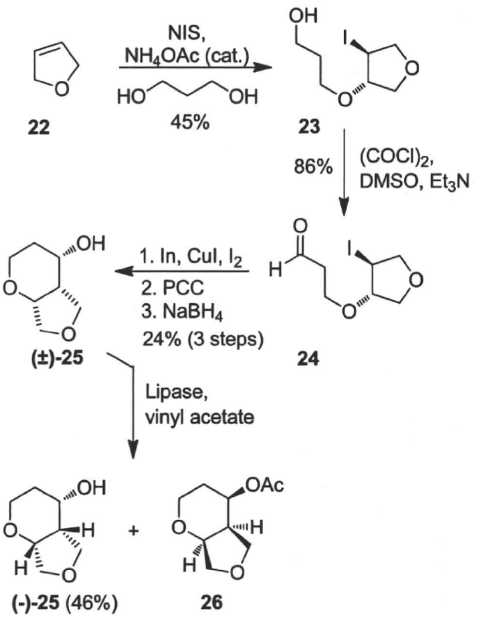

ketone provided the corresponding alcohol (dr = 10:1, as observed by ^{1}H and ^{13}C NMR). Lipase-mediated resolution of the major *cis*-alcohol gave the respective chiral ligand (−)-**19** (90% ee determined by chiral HPLC).

Since the introduction of a six-membered ring in the P_2 ligand structure may introduce more structural flexibility, we set out to explore ligands in which the cyclic oxygens were moved to adjacent positions. Such ligands would also demonstrate the importance of the oxygen positions in the bicyclic structure of ligand (−)-**7**. Thus, isomeric ligand **25** was synthesized with the furan oxygen moved to its vicinal position. The synthesis of 4-hydroxyhexahydro-2*H*-furo[3,4-*b*]pyran **25** is shown in Scheme 4. Iodoalkoxylation of the 2,5-dihydrofuran **22** using propanediol in the presence of *N*-iodosuccinimide and catalytic NH_4OAc provided iodo alcohol **23**. Swern oxidation gave aldehyde **24** in 86% yield. An intramolecular Barbier-type reaction was then conducted using indium in the presence of copper(I) iodide and iodine to furnish a mixture of diastereoisomeric alcohols.[34] Oxidation followed by stereoselective reduction using $NaBH_4$ furnished the racemic *cis,cis*-bicyclic alcohol (±)-**25** as the sole product. Lipase-mediated resolution finally gave the enantiomerically pure alcohol **25**.

To ascertain the importance of the position of the urethane in (−)-**7**, we have synthesized hexahydrofuropyran-5-ol ligand **30** shown in Scheme 5. The free hydroxyl on the pyran ring was moved to the C3 position. The synthesis was accomplished starting from enantiomerically pure bis-THF ligand **27** synthesized by us previously.[35] Dess−Martin oxidation of **27** provided the corresponding ketone. Homologation of the resulting ketone using trimethylsilyldiazomethane in the presence of $AlMe_3$ followed by treatment of the crude mixture with TBAF and acetic acid provided furanopyranone **29**. Stereoselective reduction of ketone **29** using L-selectride furnished alcohol **30** as a mixture of inseparable diastereoisomers (dr = 5:1). Both isomers were separated after formation of the corresponding activated mixed carbonate **31g**.

The synthesis of the protease inhibitors was accomplished in a two-step sequence shown in Schemes 6 and 7. Each ligand alcohol synthesized above was reacted with 4-nitrophenyl

Scheme 5. Synthesis of Hexahydrofuro[2,3-*b*]pyran-5-ol Ligand **30**

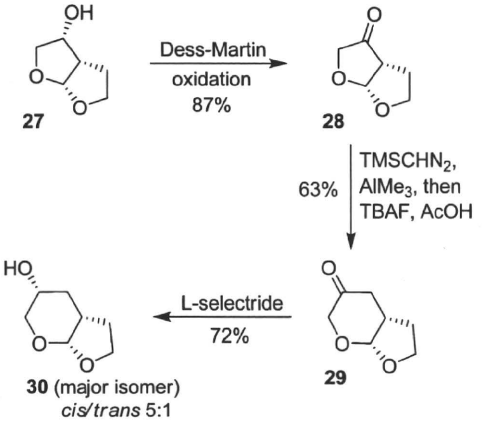

Scheme 6. Synthesis of Activated Mixed Carbonates **31a–g**

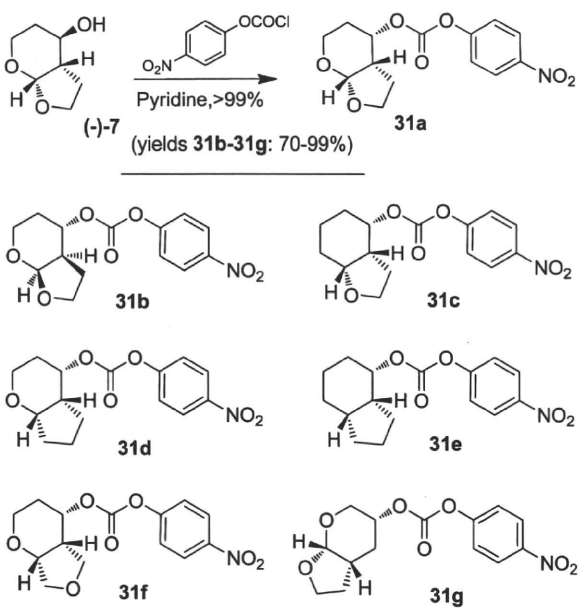

chloroformate in the presence of pyridine to form mixed activated carbonates **31a–g** in 70–99% yield. The syntheses of the corresponding protease inhibitors were achieved by coupling the mixed activated carbonates with previously reported hydroxyethylsulfonamide isosteres **32–34** (Scheme 7).[15,35] The syntheses of various HIV-PIs containing the Tp-THF (−)-**7** were achieved by respectively treating the Boc-protected isosteres **32–34** with TFA in CH_2Cl_2 and subsequently by coupling the resulting free amine isosteres with activated mixed carbonate **31a** in THF/CH_3CN in the presence of Et_3N. The corresponding inhibitors **35a**, **36**, and **37** were obtained in good yields (Scheme 7). Inhibitors **35b–g** were made in a similar manner.

Results and Discussion

As mentioned above, our preliminary modeling suggested that a hexahydrofuropyranol (−)-**7** ligand may interact with backbone atoms and residues in the protease S2-site. All inhibitors in Table 1 were evaluated in enzyme inhibitory assays following a protocol described by Toth and Marshall.[36] Inhibitors that showed potent K_i values were further evaluated through in vitro antiviral assays. As can be seen, inhibitor **35a**,

Scheme 7. Syntheses of Inhibitors **35a–g**, **36**, and **37**

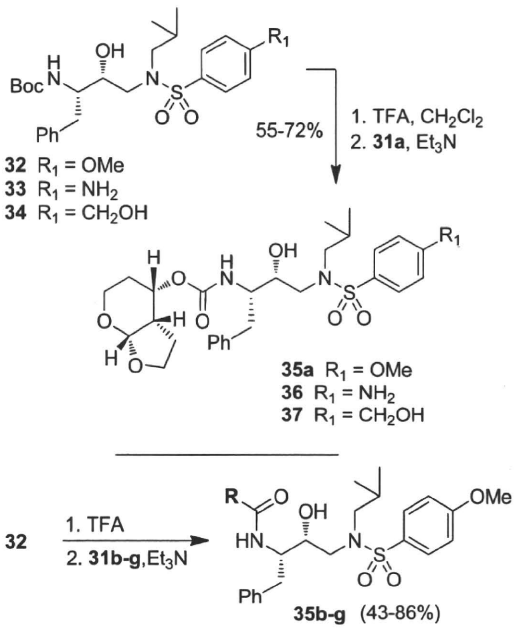

with Tp-THF (−)-**7**, exhibited an enzyme K_i value of 2.7 pM. Antiviral activity of **35a** and other inhibitors were determined in MT-2 human-T-lymphoid cells exposed to HIV-1_{LAI}.[19] As shown, **35a** has displayed remarkable antiviral potency (IC_{50} = 0.5 nM), comparable to those of PIs **1a** and **1b**. The bicyclic ring stereochemistry of the P_2 ligand proved to be important as inhibitor **35b**, with enantiomeric ligand (+)-**7**, displayed a significant reduction in enzyme inhibitory potency (> 20-fold increase in K_i) as well as antiviral activity (IC_{50} = 19 nM).

To probe the importance of the cyclic ether oxygens in the bicyclic structure of (−)-**7**, inhibitors **35c–e** were synthesized and evaluated. As shown, inhibitor **35c**, with a cyclohexane ring in place of the tetrahydropyran ring, only displayed a 2-fold reduction in K_i values but a 16-fold decrease in antiviral activity compared to inhibitor **35a**. A more dramatic loss of enzymatic potency was observed with compound **35d** with a cyclopentane ring in place of a THF ring in the P2 ligand. The K_i value dropped to 1.43 nM. Inhibitor **35e**, which lacks both cyclic ether oxygens, displayed even lower K_i and no appreciable antiviral activity. Those results clearly demonstrated the critical role of both cyclic ether oxygens in ligand (−)-**7**. Furthermore, the difference of activity observed between **35a** and **35c** suggests that the O1 oxygen on the THF-ring of (−)-**7** exerts a stronger interaction with the enzyme compared to the pyran oxygen. Inhibitor **35f**, in which the THF-oxygen of the P_2 ligand is located at a vicinal position, also exhibited a substantial loss of potency (i.e., K_i = 5.3 nM) and no antiviral activity. These results corroborated our previous observations with the bis-THF ligand in PIs **1a** and **1b**. The THF-oxygen in (−)-**7** likely has a stronger hydrogen bonding interaction with the Asp29 backbone NH and may form a weak hydrogen bond with Asp30, in the S_2 subsite of the HIV protease. We have investigated the position of the urethane oxygen on the bicyclic ligand in inhibitor **35g**. This has resulted in a substantial loss of protease inhibitory activity. Furthermore, we have examined the potency enhancing effect of the Tp-THF ligand with various hydroxyethylsulfonamide isosteres to give inhibitors **36** and **37**. The 4-methoxysulfonamide derivative **35a** appears to be the most potent inhibitor in

Table 1. Enzymatic Inhibitory and Antiviral Activity of Compounds **35a–g**, **36**, and **37**[b]

Entry	Inhibitor	K_i (nM)	IC_{50} (μM)[a]
1	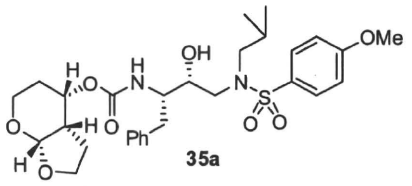 **35a**	0.0027	0.0005
2	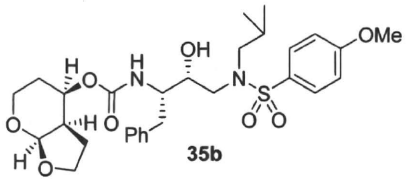 **35b**	0.068	0.019
3	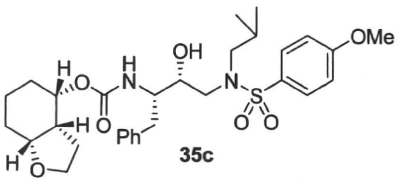 **35c**	0.005	0.008
4	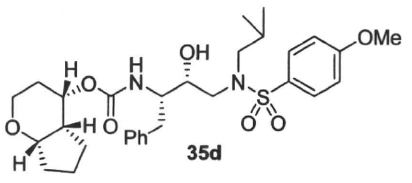 **35d**	1.43	--
5	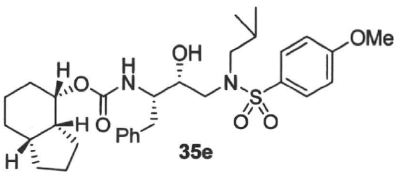 **35e**	9	>1 μM
6	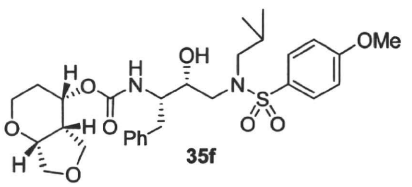 **35f**	5.3	>1 μM
7	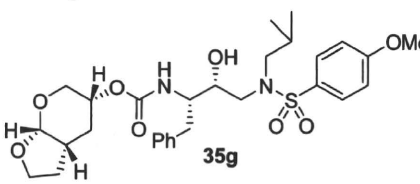 **35g**	0.11	--
8	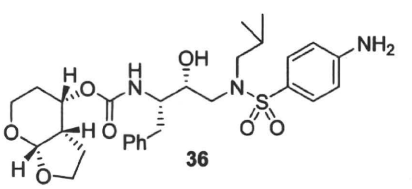 **36**	0.010	0.0065
9	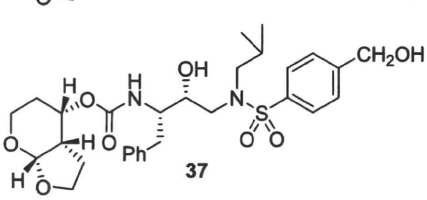 **37**	0.085	0.0045

[a] Values are the mean of at least two experiments. [b] Human T-lymphoid (MT-2) cells (2×10^3) were exposed to 100 $TCID_{50}$ of HIV-1_{LAI} and cultured in the presence of each PI, and IC_{50} values were determined using the MTT assay. The IC_{50} values of amprenavir (APV), saquinavir (SQV), and indinavir (IDV) were 0.03, 0.015, and 0.03 μM, respectively.

Table 2. Comparison of the Antiviral Activity of **35a** and Other PIs against Multidrug Resistant Clinical Isolates in PHA-PBMs Cells[a]

virus	EC_{50} (μM)			
	35a	ATV	LPV	DRV (**1a**)
HIV-$1_{ERS104pre}$ (X4)	0.0019 ± 0.0015	0.0027 ± 0.0006	0.031 ± 0.004	0.004 ± 0.001
HIV-$1_{MDR/B}$ (X4)	0.0145 ± 0.0001 (8)	0.470 ± 0.007 (174)	> 1 (> 32)	0.034 ± 0.008 (9)
HIV-$1_{MDR/C}$ (X4)	0.0037 ± 0.0018 (2)	0.039 ± 0.003 (14)	0.437 ± 0.004 (14)	0.009 ± 0.005 (2)
HIV-$1_{MDR/G}$ (X4)	0.0026 ± 0.0004 (1)	0.019 ± 0.008 (7)	0.181 ± 0.023 (6)	0.026 ± 0.009 (7)
HIV-$1_{MDR/TM}$ (X4)	0.0275 ± 0.0055 (14)	0.075 ± 0.003 (28)	0.423 ± 0.082 (14)	0.022 ± 0.015 (6)
HIV-$1_{MDR/MM}$ (R5)	0.0050 ± 0.0023 (3)	0.205 ± 0.024 (76)	0.762 ± 0.115 (25)	0.017 ± 0.005 (4)
HIV-$1_{MDR/JSL}$ (R5)	0.0275 ± 0.0009 (14)	0.293 ± 0.099 (109)	> 1 (> 32)	0.023 ± 0.005 (6)

[a] The amino acid substitutions identified in the protease-encoding region of HIV-$1_{ERS104pre}$, HIV-1_B, HIV-1_C, HIV-1_G, HIV-1_{TM}, HIV-1_{MM}, HIV-1_{JSL} compared to the consensus type B sequence cited from the Los Alamos database include L63P; L10I, K14R, L33I, M36I, M46I, F53I, K55R, I62V, L63P, A71V, G73S, V82A, L90M, I93L; L10I, I15V, K20R, L24I, M36I, M46L, I54V, I62V, L63P, K70Q,V82A, L89M; L10I, V11I, T12E, I15V, L19I, R41K, M46L, L63P, A71T, V82A, L90M; L10I, K14R, R41K, M46L, I54V, L63P, A71V, V82A, L90M; I93L, L10I, K43T, M46L, I54V, L63P, A71V, V82A, L90M, Q92K; and L10I, L24I, I33F, E35D, M36I, N37S, M46L, I54V, R57K, I62V, L63P, A71V, G73S, V82A, respectively. HIV-$1_{ERS104pre}$ served as a source of wild-type HIV-1. The EC_{50} values were determined by using PHA-PBMs as target cells, and the inhibition of p24 Gag protein production by each drug was used as an end point. The numbers in parentheses represent the fold changes of EC_{50} values for each isolate compared to the EC_{50} values for wild-type HIV-$1_{ERS104pre}$. All assays were conducted in duplicate, and the data shown represent mean values (±1 standard deviations) derived from the results of two or three independent experiments.

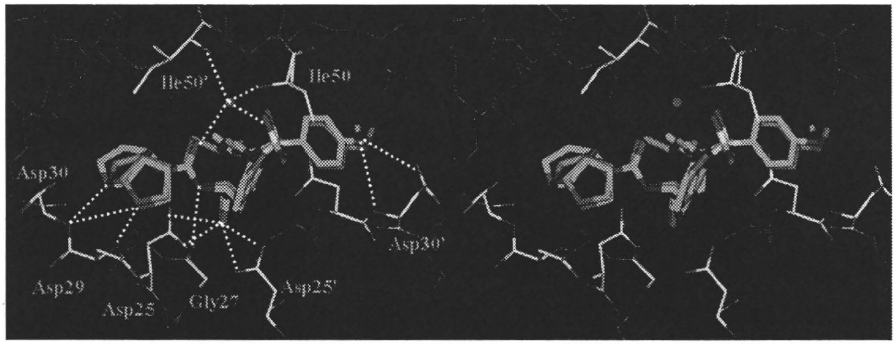

Figure 2. Stereoview of inhibitor **35a** modeled into the active site of HIV-1 protease and superimposed on the X-ray crystal structure of **1b** (PDB code 3I7E).

the series comparable to inhibitor **2**. However, the 4-amino derivative **36** exhibited very comparable enzyme inhibitory and antiviral potency similar to **1a**.

We have examined inhibitor **35a** for its activity against a panel of multidrug-resistant HIV-1 variants and compared it with that of other clinically available PIs including **1a**. The results are shown in Table 2. All inhibitors showed high antiviral activity against an HIV-1 clinical strain isolated from a drug-naive patient (wild-type).[19] Compound **35a** displayed the most potent activity with an EC_{50} of 1.9 nM. When tested against multidrug-resistant HIV-1 variants, compound **35a** retained impressively high activity to all variants with EC_{50} values ranging from 2.6 to 27.5 nM. In contrast, other inhibitors, except **1a**, exhibited substantial loss of activity. Interestingly, **1a** and **35a** showed similar fold-change of EC_{50} against most multidrug-resistant HIV strains. The results indicated that **35a** is highly active against multidrug-resistant HIV-1 variants. This inhibitor outperformed the clinically available PIs with exceedingly high antiviral activity and compared well with **1a**, which currently stands as the leading PI for the treatment of drug-resistant HIV infection.

In order to obtain molecular insights into the enzyme–inhibitor interactions of **35a** in the protease active site, an active model of **35a** was created. A stereoview of the overlaid structure of **35a** with the X-ray structure of inhibitor **1b**-bound HIV-1 protease is shown in Figure 2. Inhibitor **35a** was modeled starting from the X-ray crystal structure of **1b**. The conformation of **35a** was optimized using the MMFF94 force field,[37] as implemented in Molecular Operating Environment (version 2009.10, Chemical Computing Group, Montreal, Canada). The modeled structure maintains the important binding interactions (hydroxyl group with Asp25 and Asp25′ carboxylates; cyclic ether oxygens with Asp29 and Asp30 backbone NH bonds; methoxy oxygen with the Asp30′ backbone NH bond; carbonyl oxygen and sulfonamide oxygen with a water molecule binding to Ile50 and Ile50′) that are observed in the crystal structure of **1b**-bound HIV-1 protease.

Conclusions

We have reported the structure-based design of novel HIV-1 protease inhibitors incorporating a stereochemically defined 4-hexahydrofuropyranol-derived urethanes as the P2-ligand. The inhibitors were designed to make extensive interactions including hydrogen bonding with the protein backbone of the HIV-1 protease active site. The synthesis of (3a*S*,4*S*,7a*R*)-hexahydro-2*H*-furo[2,3-*b*]pyran-4-ol [(−)-**7**, Tp-THF] was carried out in optically active form using (3a*R*,6a*S*)-3,3a,6,6a-tetrahydro-2*H*-cyclopenta[*b*]furan-2-one as the starting material. Inhibitor **35a** has shown excellent enzyme inhibitory activity and antiviral potency comparable to that of approved PI **1a**. Furthermore, it has shown excellent activity against multi-PI-resistant variants, superior to other FDA approved inhibitors examined. The data are comparable to those of **1a**. We have carried out detailed structure–activity studies that indicated that the stereochemistry of the Tp-THF ligand and position of its oxygens are critical to the ligand's high enzyme affinity.

An active model of **35a** was created based upon the X-ray crystal structure of **1b**-bound HIV-1 protease. The overlaid structures revealed that both oxygens of the Tp-THF ligand can interact with the Asp29 and Asp30 backbone NHs, similar to the bis-THF ligand oxygens. Furthermore, the extra methylene unit in the Tp-THF ligand appears to fill in the hydrophobic pocket in the S2-site more effectively compared to the bis-THF in **1a**. The design of an inhibitor targeting the protein backbone may serve as an important guide to combat drug resistance. Further design and chemical modifications are currently underway.

Experimental Section

General Experimental Methods. All anhydrous solvents were obtained according to the following procedures: diethyl ether and tetrahydrofuran (THF) were distilled from sodium/benzophenone under argon; toluene, methanol, acetonitrile, and dichloromethane were distilled from calcium hydride; benzene was distilled from sodium. Other solvents were used without purification. All moisture-sensitive reactions were carried out in flame-dried flasks under argon atmosphere. Reactions were monitored by thin layer chromatography (TLC) using Silicycle 60A-F254 silica gel precoated plates. Flash column chromatography was performed using Silicycle 230−400 mesh silica gel. Yields refer to chromatographically and spectroscopically pure compounds. Optical rotations were recorded on a Perkin-Elmer 341 polarimeter. ^{1}H NMR and ^{13}C NMR spectra were recorded on a Varian Inova-300 (300 and 75 MHz), Bruker Avance ARX- 400 (400 and 100 MHz), or DRX-500 (500 and 125 MHz). High and low resolution mass spectra were carried out by the Mass Spectroscopy Center at Purdue University. The purity of all test compounds was determined by HRMS and HPLC analysis in the different solvent systems. All test compounds showed ≥95% purity.

(1*S*,2*R*)-2-[1-(*tert*-Butyldimethylsilyloxy)cyclopent-3-en-2-yl]-ethyl Acetate (5). To a stirred suspension of lithium aluminum hydride (93 mg, 2.45 mmol) in dry Et_2O (6 mL) was added dropwise a solution of (−)-(1*S*,5*R*)-2-oxabicyclo[3.3.0]oct-6-en-3-one (**4**) (150 mg, 1.19 mmol) in Et_2O (4 mL + 1 mL rinse) at 0 °C under argon. The reaction mixture was vigorously stirred at this temperature for 1.5 h. Water (0.1 mL) was then carefully added followed by addition of 3 M NaOH (0.1 mL) and then water (0.3 mL). The solution was stirred until formation of a white precipitate was complete. EtOAc (3 mL) and then Na_2SO_4 were added, and the resulting suspension was filtered out. The amorphous solid was washed several times with EtOAc (5 × 5 mL). The combined organic layers were dried over Na_2SO_4, filtered, and concentrated in vacuo. The crude oil was purified by flash chromatography on silica gel using hexanes/EtOAc (1:1) as the eluent to give the resulting diol (145 mg, 95%) as a colorless oil. TLC: R_f = 0.28 (hexanes/EtOAc = 1:2). ^{1}H NMR ($CDCl_3$, 300 MHz) δ 5.74 (m, 1H), 5.56 (m, 1H), 4.48 (dt, J = 2.4, 6.6 Hz, 1H), 3.84 (m, 1H), 3.71 (ddd, J = 3.6, 8.7, 10.0 Hz, 1H), 2.75 (m, 1H), 2.67 (m, 1H), 2.36 (d, J = 17.1 Hz, 1H), 1.98−1.75 (m, 1H).

To a stirred solution of the diol (76 mg, 0.59 mmol) in CH_2Cl_2 (3 mL) was added 2,4,6-collidine (1.2 mmol, 155 μL) followed by acetyl chloride (50 μL, 0.71 mmol) at −78 °C under argon. The resulting solution was stirred at this temperature for 5 h at which point additional acetyl chloride (0.25 μL, 0.24 mmol) was added. The solution was stirred for 2 h, and then saturated aqueous $NaHCO_3$ solution was added. The two layers were separated, and the aqueous layer was washed with CH_2Cl_2 (3 × 5 mL). The combined organic layer was dried over Na_2SO_4, filtered, and concentrated in vacuo. The crude oil was purified by flash chromatography on silica gel using hexanes/EtOAc (6:1, then 4:1) as the eluent to give the monoacetate (88 mg, 87%) as a colorless oil. TLC: R_f = 0.26 (hexanes/EtOAc = 2:1). ^{1}H NMR ($CDCl_3$, 300 MHz) δ 5.80−5.72 (m, 1H), 5.64−5.58 (m, 1H), 4.40 (dt, J = 2.4, 5.6 Hz, 1H), 4.20 (t, J = 7.2 Hz, 2H), 2.74−2.56 (m, 2H), 2.33 (d, J = 17.1 Hz, 1H), 2.06 (s, 3H), 2.04−1.88 (m, 1H), 1.87−1.73 (m, 1H). ^{13}C NMR ($CDCl_3$, 75 MHz) δ 171.1, 132.4, 128.4, 72.7, 63.9, 47.2, 42.1, 26.8, 21.0. HRMS-ESI (m/z): $[M + H]^+$ calcd for $C_9H_{15}O_3$ 171.1021; found 171.1020.

To a stirred solution of the above acetate (54 mg, 0.32 mmol) and 2,6-lutidine (74 μL, 0.63 mmol) in CH_2Cl_2 (1 mL) was added *tert*-butyldimethylsilyl trifluoromethanesulfonate (125 mg, 108 μL) at −78 °C under argon. The mixture was stirred for 10 min, at which point reaction completion was observed. Saturated aqueous $NaHCO_3$ solution (1 mL) and additional CH_2Cl_2 (2 mL) were added. The two layers were separated, and the aqueous layer was further extracted with CH_2Cl_2 (2 × 2 mL). The combined organic layer was washed with brine, dried ($MgSO_4$), filtered, and concentrated under reduced pressure. The crude oil was purified by column chromatography on silica gel using hexanes/EtOAc (20:1) as the eluent to afford silylated product **5** (90 mg, > 99%) as a colorless oil. TLC: R_f = 0.68 (hexanes/EtOAc = 3:1). ^{1}H NMR ($CDCl_3$, 300 MHz) δ 5.68 (s, 2H), 4.45 (dt, J = 5.1, 6.3 Hz, 1H), 4.14 (t, J = 6.9 Hz, 2H), 2.67−2.55 (m, 1H), 2.47 (dd, J = 6.9, 15.4 Hz, 1H), 2.23 (dd, J = 4.8, 15.4 Hz, 1H), 2.04 (s, 3H), 2.01−1.85 (m, 1H), 1.72−1.56 (m, 1H), 0.88 (s, 9H), 0.06 (s, 6H). ^{13}C NMR ($CDCl_3$, 75 MHz) δ 171.2, 132.7, 128.4, 73.6, 63.8, 45.9, 41.0, 27.4, 25.8, 21.0, 18.1, −4.6, −5.0.

(4*S*,4a*S*,7a*R*)-4-(*tert*-Butyldimethylsilyloxy)hexahydrofuro-[2,3-*b*]pyrane (6). To a stirred solution of **5** (76 mg, 0.27 mmol) in MeOH (2 mL) was added K_2CO_3 (37 mg, 0.27 mmol). The solution was stirred at 23 °C for 2 h. Then saturated aqueous NH_4Cl solution (2 mL) was added to the mixture. EtOAc was added, and the two layers were separated. The aqueous layer was extracted with EtOAc (4 × 3 mL). The combined organic layer was washed with brine, dried (Na_2SO_4), filtered, and concentrated under reduced pressure. The resulting oil was purified by flash chromatography on silica gel using hexanes/EtOAc (7:1) as the eluent to give the corresponding alcohol (64 mg, 98%) as a colorless oil. This intermediate was used immediately for the subsequent reaction. TLC: R_f = 0.29 (hexanes/EtOAc = 5:1). ^{1}H NMR ($CDCl_3$, 300 MHz) δ 5.72.5.62 (m, 2H), 4.52 (dt, J = 6.0, 6.9 Hz, 1H), 3.74−3.60 (m, 2H), 2.80−2.68 (m, 1H), 2.49 (ddt, J = 1.8, 7.2, 16.3 Hz, 1H), 2.34−2.29 (m, 1H), 2.06 (br s, 1H), 1.90−1.62 (m, 2H). ^{13}C NMR ($CDCl_3$, 75 MHz) δ 132.9, 128.3, 74.0, 61.1, 46.5, 40.6, 31.2, 25.8, 18.2, −4.7, −5.0.

A stream of ozonized oxygen was bubbled through a solution of the above alcohol (63.8 mg, 0.26 mmol) in CH_2Cl_2 (15 mL) at −78 °C until the blue color persisted (5 min). After the solution was flushed with nitrogen, Me_2S (0.5 mL) was added. The solution was warmed to 0 °C and stirred over a 2 h period following which anhydrous Na_2SO_4 was added. The solution was left at room temperature overnight and then filtered and concentrated in vacuo. The resulting solid was quickly passed through a short column of silica gel using hexanes/EtOAc (3:1) as the eluent to afford the hemiacetal (99 mg) as a white-solid mixture of isomers which was submitted directly to the next step. TLC: R_f = 0.26 (hexanes/EtOAc = 3:1). To an ice-cold solution of the crude diacetal (~0.25 mmol) and Et_3SiH (0.16 mL, 1.0 mmol) in CH_2Cl_2 (3 mL) under argon, was slowly added BF_3-Et_2O (60 μL, 0.5 mmol). The mixture was stirred at 0 °C for 10 min. Saturated aqueous $NaHCO_3$ solution (2 mL) and additional CH_2Cl_2 were added. The two phases were separated and the aqueous layer was further extracted with CH_2Cl_2 (3 × 2 mL). The combined organic layer was washed with brine, dried ($MgSO_4$), filtered, and concentrated in vacuo. The crude oil was purified by column chromatography on silica gel using hexanes/EtOAc (7:1) as the eluent to give bicyclic acetal **6** (38 mg, 55% 3 steps) as an amorphous solid. TLC: R_f = 0.50 (hexanes/EtOAc = 3:1). ^{1}H NMR ($CDCl_3$, 300 MHz) δ 4.95 (d, J = 3.4 Hz, 1H), 4.24−4.08 (m, 2H), 3.92 (dt, J = 8.1, 9.1 Hz, 1H), 3.85 (ddd, J = 2.0, 4.5, 12.2 Hz, 1H), 3.30 (dt, J = 2.0, 12.3 Hz, 1H), 2.39 (m, 1H), 2.07 (tt, J = 9.4, 12.0 Hz, 1H), 1.91−1.66 (m, 2H), 1.58−1.48 (m, 1H), 0.89 (s, 9H), 0.07 (s, 3H), 0.067 (s, 3H). ^{13}C NMR ($CDCl_3$, 75 MHz) δ 101.2, 68.4, 67.8, 61.1, 47.2, 30.3, 25.7, 22.4, 18.2, −4.6, −4.8.

(3a*S*,4*S*,7a*R*)-Hexahydro-2*H*-furo[2,3-*b*]pyran-4ol [(−)-7]. Bicyclic compound **6** (36 mg, 0.139 mmol) was dissolved in

THF (1 mL), and tetrabutylammonium fluoride (1 M solution THF, 0.21 mL, 0.21 mmol) was added to the solution. The mixture was stirred for 2 h at 23 °C. Saturated aqueous NH_4Cl solution was added (2 mL), followed by EtOAc (2 mL). The two phases were separated, and the aqueous layer was further extracted with EtOAc (4 × 3 mL). The combined organic layer was washed with brine, dried (Na_2SO_4), filtered, and concentrated in vacuo. The resulting compound was purified by flash chromatography on silica gel using hexanes/EtOAc (1:2 then 1:3) as the eluent to afford pure alcohol (−)-**7** (19 mg, 94%) as an amorphous solid. TLC: R_f = 0.15 (hexanes/EtOAc = 1:3). $[\alpha]_D^{23}$ −29.6 (*c* 1.06, $CHCl_3$). ^1H NMR ($CDCl_3$, 300 MHz) δ 4.99 (d, J = 2.7 Hz, 1H), 4.25−4.16 (m, 2H), 3.96 (q, J = 7.5 Hz, 1H), 3.90 (ddd, J = 2.4, 4.8, 12.3 Hz, 1H), 3.34 (td, J = 3.0, 11.7 Hz, 1H), 2.58−2.45 (m, 1H), 2.14−1.98 (m, 1H), 1.96−1.82 (m, 1H), 1.80−1.62 (m, 2H). ^{13}C NMR ($CDCl_3$, 75 MHz) δ 101.4, 68.4, 67.5, 61.0, 46.3, 29.4, 21.8. HRMS-CI (*m*/*z*): $[M + H]^+$ calcd for $C_9H_{15}O_3$ 127.0759; found 127.0757.

(3a*R*,4*R*,7a*S*)-Hexahydro-2*H*-furo[2,3-*b*]pyran-4-ol [(+)-7]. Cyclopentenediol **8** was prepared as described previously.[27b] The same synthetic sequence was the applied on the diol as for the synthesis of (−)-**7**. Ligand (+)-**7** was obtained in high enantiomeric purity [99% ee, $[\alpha]_D^{23}$ +22.3 (*c* 0.22, $CHCl_3$)].

2-Ethoxy-2,3,6,7-tetrahydrobenzofuran-4(5*H*)-one (10). To a stirred solution of 2-diazo-1,3-cyclohexanedione (300 mg, 2.17 mmol) in freshly distilled ethyl vinyl ether (5 mL) was added $[Rh_2(OAc)_4]$ (10 mg, 0.02 mmol). The mixture was stirred at room temperature for 5 h, after which the reaction was diluted with Et_2O and a few drops of pyridine were added. A red precipitate formed. The solution was filtered on a short pad of silica, flushing with Et_2O/THF (4:1) as eluent. After evaporation, the residue was purified by column chromatography on silica gel using hexanes/CH_2Cl_2/THF (8:1:1) as the eluent to furnish benzofuranone derivative **17** (347 mg, 88%). TLC: R_f = 0.29 (hexanes/EtOAc = 1:1). ^1H NMR ($CDCl_3$, 400 MHz) δ 5.72 (dd, J = 3.3, 7.4 Hz, 1H), 3.88 (m, 1H), 3.62 (m, 1H), 2.92 (ddt, J = 2.2, 7.4, 15.8 Hz, 1H), 2.70−2.62 (m, 1H), 2.52−2.37 (m, 2H), 2.33 (t, J = 6.5 Hz, 2H), 2.12−1.95 (m, 2H), 1.24 (t, J = 7.1 Hz, 3H). ^{13}C NMR ($CDCl_3$, 100 Hz) δ 195.2, 175.7, 112.3, 108.5, 65.0, 36.3, 32.7, 23.8, 21.5, 14.9.

2-Ethoxyhexahydrobenzofuran-4(2*H*)-one (11). To a solution of the ketone **10** (140 mg, 0.77 mmol) in EtOAc (9 mL) was added 5% Pd/C (128 mg, 60 μmol), and the mixture was stirred under H_2 (1 atm) for 1.5 h at room temperature. The mixture was then filtered on Celite and the pad washed with EtOAc. Evaporation of the solvent furnished the corresponding crude ketone **11** as an essentially pure mixture of diastereoisomers (130 mg, dr = 9:1). The ketone was directly submitted to the next step without purification. TLC major isomer: R_f = 0.35 (hexanes/EtOAc = 2:1).

***cis*-Octahydrobenzofuran-4-ol [(±)-12].** A solution of ketone **11** (130 mg, ca. 0.7 mmol) in CH_2Cl_2 (10 mL) was cooled to −78 °C under Ar. L-Selectride (1 M solution, 0.9 mL, 0.9 mmol) was slowly added to the solution over 5 min and the reaction mixture was stirred for 1.5 h at −78 °C. Upon complete conversion, Et_3SiH (0.6 mL, 437 mg, 3.7 mmol) was added followed by dropwise addition of TMSOTf (380 μL, 466 mg, 2.1 mmol). The solution was stirred for 2.5 h while slowly warming to 0 °C. The reaction was quenched by addition of saturated aqueous $NaHCO_3$ solution (5 mL). The two phases were separated, and the aqueous phase was extracted with Et_2O (5×). The combined organic layer was washed with brine, dried ($MgSO_4$), and evaporated under vacuum. The residue was purified by column chromatography on silica gel using hexanes/EtOAc (3:1 to 2:1) as the eluent to yield the desired alcohol (±)-**12** (78 mg, 71% over two steps) as a colorless oil. TLC: R_f = 0.25 (hexanes/EtOAc = 1:2). ^1H NMR ($CDCl_3$, 400 MHz) δ 4.01 (dt, J = 4.6, 8.8 Hz, 1H), 3.88−3.82 (m, 2H), 3.78 (dt, J = 7.1, 8.7 Hz, 1H), 2.31 (m, 1H), 2.12−1.90 (m, 2H), 1.74−1.50 (m, 5H), 1.32−1.22 (m, 1H). ^{13}C NMR ($CDCl_3$, 100 Hz) δ 77.6, 69.1, 66.7, 43.2, 30.2, 26.9, 25.9, 16.2.

(3a*S*,4*S*,7a*R*)-Octahydrobenzofuran-4-ol [(−)-12]. Racemic alcohol **12** (70 mg, 0.5 mmol) was dissolved in THF (5 mL), and vinyl acetate (120 μL, 1.25 mmol) was added. Amano lipase PS-30 (30 mg) was added, and the resulting suspension was stirred at 15−17 °C. After 48 h, 30 mg of additional enzyme was added and the mixture was left for additional 48 h until ~54% conversion was reached (NMR and GC). The resulting suspension was diluted with Et_2O and filtered on Celite and the filter cake rinsed with Et_2O. After evaporation of the remaining solvent, the residue was purified by column chromatography using hexanes/EtOAc (5:1, 3:1, then 2:1) as the eluent to yield acetyl furanol **13** (38 mg, 41%) and the desired enantioenriched (−)-hexahydrobenzofuranol (−)-**12** (24 mg, 35%). The enantiomeric excess of the 2,4-dinitrobenzoate derivative of (−)-**12** was determined to be 98.8% ee by chiral HPLC: column ChiralPak IA, hexane/isopropanol (90/10 to 50/50, 40 min), 1 mL/min, 35 °C, λ = 254 nm, t_R major = 16.54 min, t_R minor = 37.1 min.

2-[3-(*tert*-Butyldimethylsilyl)oxy)-1-hydroxypropyl]cyclopentanone (15). A solution of lithium diisopropylamide (14 mmol), freshly prepared by adding *n*-BuLi (1.6 M solution in hexanes, 8.75 mL, 14 mmol) to diisopropylamine (1.97 mL, 1.42 g, 14 mmol) in THF (30 mL) at 0 °C under argon followed by stirring for 30 min, was cooled to −78 °C, and cyclopentanone **14** (1.12 mL, 1.07 g, 12.7 mmol) in THF (5 mL) was added dropwise over 10 min. After being stirred at −78 °C for 1.5 h, 3-*tert*-butyldimethylsilyloxypropionaldehyde (1.55 g, 8.2 mmol) in THF (20 mL) was added dropwise over 5 min. The mixture was stirred for an additional 2 h, and the reaction was quenched by addition of saturated aqueous NH_4Cl solution (10 mL). Following dilution with Et_2O, the two phases were separated, and the aqueous phase was extracted with Et_2O (2×). The combined organic phase was washed with brine, dried ($MgSO_4$), filtered, and evaporated. The residue was quickly purified by column chromatography on silica gel using hexanes/EtOAc (20:1 to 10:1) as the eluent to give **15** as a 3:1 mixture of diastereoisomers (2.13 g, 95%). Light yellow oil. TLC: R_f = 0.37 and 0.23 (hexanes/EtOAc = 5:1). ^1H NMR ($CDCl_3$, 400 MHz) δ 4.27 (dt, J = 3.1, 9.3 Hz, 0.3H), 4.10 (s, 1H), 3.91 (m, 1H), 3.87 (m, 0.3H), 3.85−3.75 (m, 2.6H), 2.38−2.30 (m, 6.5H), 1.80−1.56 (m, 5.2H), 0.88 (brs, 12H), 0.06 (s, 2H), 0.05 (s, 6H). ^{13}C NMR ($CDCl_3$, 100 MHz) δ 222.8, 220.4, 70.4, 70.2, 62.6, 60.5, 54.5, 53.9, 39.1, 38.7, 37.0, 36.6, 26.4, 25.9, 25.8, 23.5, 20.7, 20.5, 18.2, −5.5, −5.6. HRMS-CI (*m*/*z*): $[M - OH]^+$ calcd for $C_{14}H_{27}O_2Si$ 255.1780; found 255.1785.

2,3,6,7-Tetrahydrocyclopenta[*b*]pyran-4(5*H*)-one (16). To a solution of DMSO (425 μL, 468 mg, 6 mmol) in CH_2Cl_2 (3 mL) was added $(CF_3CO)_2O$ (406 μL, 609 mg, 2.9 mmol) dropwise at −78 °C under argon. The resulting mixture was stirred at that temperature for 45 min. Then a precooled solution of ketone **15** (272 mg, 1 mmol) in CH_2Cl_2 (3 mL) was added. The reaction mixture was stirred at −78 °C for 30 min, then at −15 °C for 15 min and cooled back to −78 °C. Et_3N (1.25 mL, 911 mg, 9 mmol) was added, and the mixture was stirred at −78 °C for 45 min. The reaction was quenched by addition of saturated aqueous NH_4Cl solution and the mixture warmed to room temperature. The two phases were separated and the aqueous phase was extracted with CH_2Cl_2 (3×) and then EtOAc (1×). The combined organic phase was washed with brine, dried (Na_2SO_4), filtered, and concentrated under reduced pressure. The residue was purified by flash column chromatography using hexanes/EtOAc (20:1, then 15:1 with a few drops of acetic acid) as the eluent to give the corresponding diketone (221 mg, 82%) as a light orange oil. TLC: R_f = 0.37 (hexanes/EtOAc = 10:1). ^1H NMR ($CDCl_3$, 400 MHz) δ 12.7 (br s, 1H), 3.90 (t, J = 6.2 Hz, 0.66H), 3.89 (t, J = 6.5 Hz, 2H), 3.46 (t, J = 7.8 Hz, 0.33H), 2.86 (dt, J = 3.0, 6.2 Hz, 0.66H), 2.58 (t, J = 7.2 Hz, 2H), 2.45 (t, J = 6.5 hz, 2H), 2.40 (t, J = 7.9 Hz, 2H), 2.31−2.19 (m, 0.66H), 2.10−1.97 (m, 0.66H), 1.95−1.82 (m, 2H), 0.86 (s, 9H), 0.86 (s, 3H), 0.04 (s, 1H), 0.03 (s, 1H), 0.03 (s, 6H). ^{13}C NMR ($CDCl_3$, 100 MHz) δ 212.9, 206.1, 203.6, 175.4, 110.9, 62.4, 59.6, 58.5, 45.6, 38.7, 37.8, 37.0, 25.7, 25.6, 25.0, 20.6, 20.3, 18.1, −5.6. HRMS-CI (*m*/*z*): $[M + H]^+$ calcd for $C_{14}H_{26}O_3Si$ 271.1729; found 271.1733.

Diketone (54 mg, 0.2 mmol) was dissolved in CH_2Cl_2 (2 mL) and cooled to 0 °C under argon. Trifluoroacetic acid (90 μL, 134 mg, 1.2 mmol) was then added dropwise. The mixture was stirred at 0 °C for 30 min and then warmed to room temperature and stirred for 4 h. As completion was reached, solid $NaHCO_3$ (~150 mg) was then added and the mixture diluted with EtOAc. After being stirred for 10 min, the suspension was filtered on a small Celite pad. The solvent was evaporated under reduced pressure and the residue purified by column chromatography on silica gel using hexanes/EtOAc (4:1) as the eluent to furnish α,β-unsaturated ketone **16** (26 mg, 94%) as a colorless oil. TLC: R_f = 0.23 (hexanes/EtOAc = 3:1). ^{1}H NMR ($CDCl_3$, 400 MHz) δ 4.49 (t, J = 6.9 Hz, 2H), 2.59−2.45 (m, 6H), 1.89 (m, 2H). ^{13}C NMR ($CDCl_3$, 100 MHz) δ 189.6, 178.5, 114.5, 69.5, 35.4, 32.6, 25.6, 19.0.

Octahydrocyclopenta[*b*]pyran-4-ol [(±)-18]. A solution of α,β-unsaturated ketone **16** (109 mg, 0.79 mmol) in EtOAc (6 mL) was loaded with 10% Pd/C (50 mg, 0.047 mmol) and carefully placed under H_2 (1 atm). The mixture was stirred at room temperature for 12 h. The suspension was then filtered over a Celite pad, the pad washed with EtOAc, and the resulting solution evaporated under reduced pressure. The essentially pure ketone (81 mg) was directly carried out to the next step without further purification. TLC: R_f = 0.37 (hexanes/EtOAc = 3:1). ^{1}H NMR ($CDCl_3$, 400 MHz) δ 4.22−4.15 (m, 2H), 3.69 (td, J = 2.8, 12.0 Hz, 1H), 2.71 (ddd, J = 7.2, 12.3, 15.7 Hz, 1H), 2.48 (dt, J = 4.0, 9.0 Hz, 1H), 2.23 (ddt, J = 1.4, 2.8, 15.7 Hz, 1H), 2.00−1.80 (m, 5H), 1.71−1.63 (m, 1H). ^{13}C NMR ($CDCl_3$, 100 MHz) δ 210.2, 82.8, 65.9, 55.1, 38.5, 33.3, 28.4, 22.8.

The ketone was diluted in CH_2Cl_2 (5 mL) under argon and cooled to −78 °C. L-Selectride (1 M solution in THF, 0.80 mL, 0.8 mmol) was added dropwise, and the resulting mixture was stirred at this temperature for 2 h. Hydrogen peroxide (30% aqueous solution, 3 mL) and 3 N NaOH aqueous solution were added, and the mixture was warmed to 23 °C and stirred for 5 h. The phases were separated and the aqueous phase extracted with CH_2Cl_2 (4×). The combined organic phase was washed with brine, dried (Mg_2SO_4), filtered, and evaporated under reduced pressure. The residue was purified by column chromatography on silica gel using hexanes/EtOAc (4:1, then 1.5:1) as the eluent to yield *cis*-bicyclic alcohol (±)-**18** (77 mg, 68% two steps) as a colorless oil. TLC: R_f = 0.13 (hexanes/EtOAc = 2:1). ^{1}H NMR ($CDCl_3$, 400 MHz) δ 4.11 (dt, J = 5.6, 11.1 Hz, 1H), 3.91 (ddd, J = 2.0, 4.5, 11.7 Hz, 1H), 3.84−3.81 (m, 1H), 3.33 (dt, J = 2.3, 11.9 Hz, 1H), 2.17−2.08 (m, 1H), 1.92−1.81 (m, 1H), 1.79−1.55 (m, 7H). ^{13}C NMR ($CDCl_3$, 125 MHz) δ 80.5, 68.3, 65.4, 47.0, 32.6, 29.7, 21.6, 21.3.

(4*S*,4a*S*,7a*S*)-Octahydrocyclopenta[*b*]pyran-4-ol [(−)-18]. Racemic alcohol (±)-**18** (68 mg, 0.48 mmol) was dissolved in THF (5 mL), and vinyl acetate (225 μL, 2.4 mmol) was added. Amano lipase PS-30 (30 mg) was added, and the resulting suspension was stirred at 15−20 °C. The mixture was left stirring for >48 h until around 50% conversion was reached (as seen by NMR). The resulting suspension was diluted with Et_2O and filtered on Celite, and the filter cake was rinsed with Et_2O. After evaporation of the remaining solvent, the residue was purified by column chromatography using hexanes/EtOAc (5:1, 3:1, then 1.5:1) to yield the desired enantio enriched pyranol (−)-**18** (25 mg, 37%). $[\alpha]_D^{20}$ −47.5 (*c* 1.32, $CHCl_3$). An enantiopurity of 94.1% ee for the alcohol was measured by chiral HPLC analysis of the corresponding activated carbonate **31d**: column ChiralPak IA, 0.7 mL/min, hexanes/IPA (98:2 to 85:15, from 0 to 45 min), λ = 210 nm, T = 30 °C, t_R minor = 22.4 min, t_R major = 23.3 min.

(±)-*endo*,*cis*-Bicyclo[4.3.0]nonan-2-ol [(±)-19]. Enone **17**[33] (106 mg, 0.77 mol) was dissolved in THF (10 mL), and the flask was purged with argon. Pd/C 10% (60 mg, 0.06 mmol) was added to the solution, and the resulting suspension was stirred under hydrogen (1 atm). TLC monitoring first shows isomerization of the enone, through migration of the olefin to the internal position, followed by slow formation of the reduced cis-product. After 12 h, the solution was filtered on a pad of Celite and the solvent removed in vacuo. The residue was purifed by flash column chromatography on silica gel using hexanes/EtOAc (30:1 to 10:1) to give the reduced ketone (98 mg, 92%). TLC: R_f = 0.65 (hexanes/EtOAc = 5:1). ^{1}H NMR ($CDCl_3$, 400 MHz) δ 2.62−2.54 (m, 1H), 2.48−2.38 (m, 1H), 2.38−2.23 (m, 2H), 2.08−1.98 (m, 1H), 1.94−1.30 (m, 9H). ^{13}C NMR ($CDCl_3$, 100 MHz) δ 214.6, 53.1, 42.9, 39.6, 31.0, 27.2, 26.6, 23.8, 23.0. A solution of the ketone (135 mg, 0.98 mmol) in CH_2Cl_2 (3 mL) was cooled to −78 °C under argon. L-Selectride (1 M solution THF, 1.2 mL) was added dropwise to the solution, and the reaction mixture was stirred at −78 °C for 1 h. Hydrogen peroxide solution (30% solution, 1.5 mL) and then NaOH (3 M solution, 1.5 mL) were added, and the mixture was warmed to 23 °C and stirred for 1 h. After dilution with water (2 mL) and then addition of Na_2SO_3 saturated aqueous solution (3 mL), the aqueous phase was successively extracted with CH_2Cl_2 (4×). The combined organic phase was dried (Na_2SO_4), filtered, and evaporated in vacuo. The residue was purified by column chromatography on silica gel using hexanes/EtOAc (6:1) to yield racemic alcohol (±)-**19** (92 mg, 66%) as a colorless oil. TLC: R_f = 0.25 (hexanes/EtOAc = 5:1). ^{1}H NMR ($CDCl_3$, 500 MHz) δ 3.96 (m, 1H), 2.26−2.17 (m, 1H), 1.93 (m, 1H), 1.79−1.53 (m, 7H), 1.47−1.15 (5 H), 0.96 (dq, J = 3.3, 13.0 Hz, 1H). ^{13}C NMR ($CDCl_3$, 125 MHz) δ 71.6, 46.4, 40.1, 31.5, 29.5, 27.0, 23.9, 21.4, 21.2. HRMS-EI (*m*/*z*): $[M - OH]^-$ calcd for C_9H_{15} 122.1096, found 122.1097.

(1*R*,2*S*,6*R*)-Bicyclo[4.3.0]nonan-2-ol [(−)-19]. Racemic **19** (86 mg, 0.62 mmol) was dissolved in THF (5 mL), and vinyl acetate (0.5 mL) was added. Amano lipase PS-30 (60 mg) was added, and the resulting suspension was stirred at 23 °C until 50% conversion was reached (NMR) in ~6 h. The resulting suspension was diluted with Et_2O and filtered on Celite, and the filter cake was rinsed with Et_2O. After evaporation of the remaining solvent, the residue was purified by column chromatography using hexanes/EtOAc (8:1, 6:1, then 4:1) to yield acetate **21** and the desired enantioenriched (−)-indanol (−)-**19** (38.5 mg, 45% yield). $[\alpha]_D^{20}$ −28.3° (*c* 1.02, $CHCl_3$), ($[\alpha]_D^{20}$ lit. −27.2° (*c* 1.0, $CHCl_3$)).[38] The enantiomeric excess of the 2,4-dinitrobenzoate derivative was determined to be 89.9% ee by chiral HPLC, column ChiralPak IA, hexane/isopropanol (100/0 to 90/10, 15 min; 90/10 to 80/20, 15 min), 1 mL/min, t_R minor = 16.58 min, t_R major = 19.5 min.

3-[(4-Iodotetrahydrofuran-3-yl)oxy]propan-1-ol (23). To a solution of freshly distilled 2,5-dihydrofuran (700 mg, 0.740 mL, 10 mmol), in a mixture of dry 1,3-propanediol/dimethoxyethane (1:1, 5 mL) at 0 °C under argon was successively added NH_4OAc (77 mg, 1 mmol), followed by *N*-iodosuccinimide (11 mmol, 2.47 g). The mixture was warmed to 23 °C and stirred for 12 h protected from light. The reaction was quenched by addition of saturated aqueous Na_2SO_3 and then diluted with water. The mixture was extracted with Et_2O/EtOAc (1:1). The combined organic phase was dried (Na_2SO_4), filtered, and evaporated under reduced pressure. The residue was purified by flash column chromatography on silica gel using hexanes/EtOAc (4:1, 3:1, then 2.5:1) to give iodo alcohol **23** (1.2 g, 45%) as a pale yellow oil. TLC: R_f = 0.3 (hexanes/EtOAc = 1:1). ^{1}H NMR ($CDCl_3$, 400 MHz) δ 4.33 (m, 1H), 4.29−4.19 (m, 3H), 4.04 (dd, J = 2.2, 9.8 Hz, 1H), 3.79 (dd, J = 1.5, 9.8 Hz, 1H), 3.76−3.69 (m, 3H), 3.60 (m, 1H), 1.81 (m, 2H). ^{13}C NMR ($CDCl_3$, 100 MHz) δ 88.2, 76.1, 71.8, 67.9, 60.6, 32.3, 23.4.

3-[(4-Iodotetrahydrofuran-3-yl)oxy]propanal (24). Oxalyl chloride (580 mg, 392 μL, 4.6 mmol) was diluted in CH_2Cl_2 (12 mL) under argon, and the solution was cooled to −78 °C. Dry DMSO (715 mg, 650 μL, 9.15 mmol) in CH_2Cl_2 (3 mL) was added to the cold solution dropwise, and the mixture was stirred for 30 min. A solution of alcohol **23** (500 mg, 1.83 mmol) in CH_2Cl_2 (4 mL) was then added slowly, and the mixture was kept stirring for an additional hour at −78 °C. Et_3N (1.3 g, 1.8 mL,

12.8 mmol) was then introduced. The white suspension was stirred at −78 °C for 20 min and slowly warmed to room temperature. A 0.5 M phosphate buffer solution pH 5.5 (20 mL) was added. The two phases were separated, and the resulting aqueous phase was extracted with Et_2O (4×). The combined organic phase was dried ($MgSO_4$), filtered, and evaporated. The residue was purified by flash column chromatography using hexanes/EtOAc (6:1 to 4:1) to yield the desired aldehyde **24** (433 mg, 86%) as a light yellow oil. TLC: R_f = 0.76 (hexanes/EtOAc = 1:1). ^{1}H NMR ($CDCl_3$, 300 MHz) δ 9.77 (t, J = 1.3 Hz, 1H), 4.35 (m, 1H), 4.30−4.19 (m, 3H), 4.04 (dd, J = 2.3, 9.8 Hz, 1H), 3.92 (ddd, J = 5.3, 6.7, 9.5 Hz, 1H), 3.77 (dd, J = 1.7, 10.1 Hz, 1H), 3.75 (ddd, J = 5.2, 6.2, 9.5 Hz, 1H), 2.69 (m, 2H). ^{13}C NMR ($CDCl_3$, 75 MHz) δ 200.1, 88.3, 76.1, 71.8, 63.1, 43.7, 23.3.

Hexahydro-2*H*-furo[3,4-*b*]pyran-4-ol [(±)-25]. To a solution of aldehyde **24** (100 mg, 0.37 mmol) in DME (10 mL) was successively added indium (60 mg, 0.55 mmol), CuI (48 mg, 0.25 mmol), and a catalytic amount of iodine (10 mg, 0.037 mmol). After the suspension was stirred for 5 min, water (4 mL) was added and the mixture was stirred at room temperature for 4 h. The suspension was filtered on a Celite pad, washing the pad with THF. The solvent was reduced under vacuum and the resulting aqueous phase acidified with 1 M HCl and saturated with NaCl. The aqueous phase was extracted with EtOAc, and the combined organic phase was dried over $MgSO_4$. After filtration and evaporation, the crude was purified by flash column chromatography on silica gel using hexanes/EtOAc (1:1 to 1:5) to provide the bicyclic alcohol (±)-**25** (25 mg, 47%) as a mixture of diastereoisomers. TLC: R_f = 0.28 (EtOAc 100%). Pyridinium chlorochromate (74 mg, 0.346 mmol) was added to a suspension of flame-dried 4 Å molecular sieves in CH_2Cl_2 (2 mL) at room temperature under argon. A solution of the above alcohol (25 mg, 0.173 mmol) in CH_2Cl_2 (1.5 mL) was transferred to the suspension at 0 °C, and the solution was stirred for 1 h at 0 °C. The reaction was quenched by addition of isopropanol, and the mixture was filtered on a silica pad, flushing with Et_2O. After evaporation of the solvent, the corresponding ketone thus obtained was used directly in the next step. TLC: R_f = 0.45 (hexanes/EtOAc = 1:1). The ketone was redissolved in EtOH (1.5 mL). The solution was cooled to −20 °C, and $NaBH_4$ (25 mg, 0.66 mmol) was added at once. After being stirred at this temperature for 30 min, the reaction was quenched by addition of saturated aqueous NH_4Cl solution (1.5 mL). The solution was extracted with EtOAc and the combined organic phase dried (Na_2SO_4), filtered, and evaporated. The corresponding racemic alcohol (±)-**25** was purified by flash column chromatography using hexanes/EtOAc (1:1 to 1:5) as the eluent. Colorless oil (12 mg, 50% two steps). TLC: R_f = 0.25 (100% EtOAc). ^{1}H NMR ($CDCl_3$, 300 MHz) δ 4.26 (m, 1H), 4.05 (t, J = 3.0 Hz, 1H), 4.04−3.95 (m, 3H), 3.94−3.85 (m, 2H), 3.40 (dt, J = 2.5, 11.8 Hz, 1H), 2.60 (m, 1H), 1.94 (d, J = 4.0 Hz, 1H), 1.80 (ddt, J = 4.6, 11.5, 12.5 Hz, 1H), 1.74 (m, 1H). ^{13}C NMR ($CDCl_3$, 75 MHz) δ 78.3, 74.5, 67.1, 66.4, 65.0, 45.5, 30.0.

To a solution of racemic (±)-**25** (10 mg, 0.07 mmol) in dry THF (1 mL) under an argon atmosphere was added vinyl acetate (60 mg, 65 μL, 0.7 mmol) followed by addition of immobilized Amano Lipase PS-30 (10 mg) on Celite-545. The mixture was stirred at 15−20 °C for 2 days until >50% conversion could be observed by NMR of aliquots. The resulting suspension was diluted in Et_2O and filtered on a small Celite pad. The solvents were evaporated and the residue was purified by flash chromatography using hexanes/EtOAc (1:1 to 1:5) as the eluent to give enantiomeric alcohol **25** (4.6 mg, 46%) as a colorless oil. An enantiopurity of >99.5% ee for the alcohol was measured by analysis of the corresponding activated carbonate **31f** on chiral HPLC (column ChiralPak IC, hexane/isopropanol 52:48, 1 mL/min, λ = 215 nm, T = 24 °C, t_R minor = 14.4 min, t_R major = 15.5 min).

(3a*R*,6a*R*)-Tetrahydrofuro[2,3-*b*]furan-3(2*H*)-one (28). Enantiomerically pure (3*R*,3a*S*,6a*R*)-hexahydrofuro[2,3-*b*]furan-3-ol (bis-THF) **27** (85 mg, 0.65 mmol) was diluted in dry CH_2Cl_2 (6 mL) under argon. The solution was cooled to 0 °C, and anhydrous Na_2HPO_4 (52 mg, 0.36 mol) was added. Dess−Martin periodinane (360 mg, 0.85 mmol) was added at once at 0 °C and the resulting suspension warmed to 23 °C and stirred for 3 h. The reaction was then quenched by successive addition of saturated aqueous $NaHCO_3$ and saturated aqueous Na_2SO_3 solutions (1.5 + 1.5 mL). The phases were separated, and the aqueous phase was extracted with CH_2Cl_2 and then EtOAc. The combined organic phases were dried (Na_2SO_4), filtered on a small pad of silica gel, and evaporated to dryness. The residue was purified by column chromatography on silica gel using hexanes/EtOAc (3:1) to furnish ketone **28** (73 mg, 87%) as a white crystalline solid. TLC: R_f = 0.57 (hexanes/EtOAc = 1:1). Spectral data corresponded to those previously reported in the literature.[35]

(3a*S*,7a*R*)-Tetrahydro-2*H*-furo[2,3-*b*]pyran-5(3*H*)-one (29). $AlMe_3$ (25% w/w hexanes, 250 μL, 0.6 mmol) was diluted in dry CH_2Cl_2 (5 mL) under argon, and the solution was cooled to −78 °C. A solution of ketone **28** (64 mg, 0.5 mmol) in dry CH_2Cl_2 (5 mL) was slowly added dropwise. After 10 min, $TMSCHN_2$ (2 M solution in Et_2O, 275 μL, 0.55 mmol) was added. The mixture was stirred for 2 h while warming to −30 °C. Saturated Rochelle's salt solution (5 mL) was added, and the mixture was stirred for 1 h. The phases were separated. The aqueous phase was extracted with CH_2Cl_2, and the combined organic phase was dried ($MgSO_4$). The solution was filtered on a small silica gel pad, flushing with Et_2O, and the collected organic phase was evaporated. A crude mixture of the desired ketone along with α-silylated derivatives and isomers was then obtained. The mixture was redissolved in THF (5 mL). AcOH (6 drops) and TBAF (0.5 mL, 0.5 mmol) were successively added. The resulting mixture was stirred at 23 °C for 3 h and evaporated to dryness. The residue was purified by flash column chromatography on silica gel using hexanes/EtOAc (5:1) as the eluent to give ketone **29** (45 mg, 63%). TLC: R_f = 0.35 (hexanes/EtOAc = 2:1). ^{1}H NMR ($CDCl_3$, 400 MHz) δ 5.49 (d, J = 6.8 Hz, 1H), 4.11 (d, J = 18.2 Hz, 1H), 4.10 (m, 1H), 3.92 (d, J = 18.2 Hz, 1H), 3.74 (dt, J = 6.5, 8.9 Hz, 1H), 2.85 (m, 1H), 2.71 (d, J = 6.3, 15.6 Hz, 1H), 2.48 (d, J = 3.9, 15.6 Hz, 1H), 2.15 (m, 1H), 1.55 (ddt, J = 7.7, 8.9, 12.7 Hz, 1H). ^{13}C NMR ($CDCl_3$, 100 MHz) δ 210.7, 100.9, 67.5, 67.1, 39.2, 36.2, 31.3.

(3a*S*,5*R*,7a*R*)-Hexahydro-2*H*-furo[2,3-*b*]pyran-5-ol (30). A solution of ketone **29** (25 mg, 0.173 mmol) dissolved in CH_2Cl_2 (5 mL) was cooled to −78 °C under argon. L-Selectride (1 M in THF, 200 μL, 0.2 mmol) was added dropwise. The solution was stirred at this temperature for 3 h and quenched by addition of saturated aqueous NH_4Cl solution. The aqueous phase was extracted with EtOAc. The combined organic extract was dried (Na_2SO_4), filtered, and evaporated. The crude was purified by column chromatography on silica gel using hexanes/EtOAc (2:1, 1:1, then 1:2) to yield alcohol **30** as a 5:1 mixture of diastereoisomers (18 mg, cis major). The stereoisomers were separated in the subsequent synthesis of the mixed activated carbonate **31g**. TLC: R_f = 0.25 (hexanes/EtOAc = 1:2). ^{1}H NMR ($CDCl_3$, 300 MHz) δ 5.08 (d, J = 3.8 Hz, 0.2H), 5.05 (d, J = 3.3 Hz, 1H), 4.16−4.11 (m, 1.2H), 3.95−3.84 (m, 1.6H), 3.81−3.70 (m, 2H), 3.63 (m, 1H), 3.27 (dd, J = 7.9, 11.2 Hz, 0.2H), 2.35−1.70 (m, 6H).

(3a*S*,4*S*,7a*R*)-Hexahydro-2*H*-furo[2,3-*b*]pyran-4-yl (4-Nitrophenyl) Carbonate (31a). Furopyranol ligand (−)-7 (9 mg, 0.063 mmol) was diluted in CH_2Cl_2 (0.5 mL) under argon. The solution was cooled to 0 °C, and dry pyridine (17 μL, ~0.21 mmol) was added. 4-Nitrophenyl chloroformate (24 mg, 0.12 mmol) was added at once to the solution, upon which a white precipitate formed. The mixture was stirred for 2 h while warming to room temperature. Upon completion, the mixture was concentrated under reduced pressure and the residue was purified by column chromatography on silica gel using hexanes/EtOAc (6:1, then 3:1) as the eluent to give the corresponding

activated carbonate **31a** (18 mg, >99%). TLC: R_f = 0.25 (hexanes/EtOAc = 3:1). ^{1}H NMR ($CDCl_3$, 300 MHz) δ 8.29 (d, J = 8.7 Hz, 2H), 7.39 (d, J = 8.7 Hz, 2H), 5.30−5.19 (m, 1 H), 5.07 (d, J = 2.7 Hz, 1H), 4.28 (dt, J = 3 Hz, 1H), 4.04−3.95 (m, 2H), 3.47−3.37 (m, 1H), 2.80−2.68 (m, 1H), 2.30−2.10 (m, 1H), 2.05−1.90 (m, 3H). ^{13}C NMR ($CDCl_3$, 75 MHz) δ 155.3, 151.7, 145.4, 125.3, 121.7, 101.1, 75.4, 68.5, 60.5, 43.2, 25.8, 22.5.

(3a*R*,4*R*,7a*S*)-Hexahydro-2*H*-furo[2,3-*b*]pyran-4-yl (4-Nitrophenyl) Carbonate (31b). The title compound was obtained from (+)-**7** as described for (−)-**7** in 86% yield after purification by column chromatography on silica gel using hexanes/EtOAc (6:1, then 3:1). Spectral data were consistent with those recorded for **31a**.

(3a*R*,4*S*,7a*R*)-Octahydrobenzofuran-4-yl (4-Nitrophenyl) Carbonate (31c). The title compound was obtained from (−)-**12** as described for (−)-**7** in 83% yield after purification by column chromatography on silica gel using hexanes/EtOAc (8:1 to 6:1). TLC: R_f = 0.7 (hexanes/EtOAc = 3:1). ^{1}H NMR ($CDCl_3$, 400 MHz) δ 8.28 (d, J = 9.2 Hz, 2H), 7.39 (d, J = 9.2 Hz, 2H), 5.07 (m, 1H), 4.13−4.05 (m, 2H), 3.90 (q, J = 8.2 Hz, 1H), 2.72 (m, 1H), 2.10−2.00 (m, 2H), 1.90−1.68 (m, 4H), 1.55−1.45 (m, 1H), 1.34−1.23 (m, 1H). ^{13}C NMR ($CDCl_3$, 100 MHz) δ 155.4, 151.9, 145.2, 125.2, 121.7, 77.7, 77.1, 66.5, 41.2, 27.0, 26.2, 25.4, 18.0.

((4*S*,4a*R*,7a*S*)-Octahydrocyclopenta[*b*]pyran-4-yl) (4-Nitrophenyl) Carbonate (31d). The title compound was obtained from (−)-**18** as described for (−)-**7** in 85% yield after purification by column chromatography on silica gel using hexanes/CH_2Cl_2/THF (4:1:0 then 4:1:0.1) as the eluent. TLC: R_f = 0.31 (hexanes/EtOAc = 1:1). ^{1}H NMR ($CDCl_3$, 400 MHz) δ 8.28 (d, J = 9.1 Hz, 2H), 7.38 (d, J = 9.1 Hz, 2H), 5.21 (m, 1H), 4.00 (ddd, J = 1.8, 4.7, 12.0 Hz, 1H), 3.93 (dt, J = 2.5, 2.7 Hz, 1H), 3.43 (dt, J = 2.1, 12.0 Hz, 1H), 2.36 (m, 1H), 2.04−1.82 (m, 4H), 1.82−1.62 (m, 4H). ^{13}C NMR ($CDCl_3$, 100 MHz) δ 155.5, 151.9, 145.3, 125.3, 121.8, 80.7, 77.3, 65.0, 43.7, 32.6, 26.3, 22.3, 21.7.

(3a*R*,4*S*,7a*R*)-Octahydro-1*H*-inden-4-yl (4-Nitrophenyl) Carbonate (31e). The title compound was obtained from (−)-**19** as described for (−)-**7** in 90% yield after purification by column chromatography on silica gel using hexanes/EtOAc (20:1 to 10:1) as the eluent. ^{1}H NMR ($CDCl_3$, 400 MHz) δ 8.27 (d, J = 9.1 Hz, 2H), 7.38 (d, J = 9.1 Hz, 2H), 5.05 (m, 1H), 2.41 (m, 1H), 2.05 (m, 1H), 1.98−1.24 (m, 11H), 1.05 (dq, J = 3.4, 12.7 Hz, 1H). ^{13}C NMR ($CDCl_3$, 100 MHz) δ 155.7, 151.9, 145.2, 125.2, 121.8, 80.7, 42.8, 40.2, 31.3, 26.6, 25.7, 23.4, 22.4, 21.3.

(4*S*,4a*S*,7a*R*)-Hexahydro-2*H*-furo[3,4-*b*]pyran-4-yl (4-Nitrophenyl) Carbonate (31f). The title was obtained from (−)-**25** as described for (−)-**7** in >99% yield following column chromatography purification on silica gel using hexanes/EtOAc (3:1, then 2:1) as the eluent. ^{1}H NMR ($CDCl_3$, 400 MHz) δ 8.29 (d, J = 9.1 Hz, 2H), 7.38 (d, J = 9.1 Hz, 2H), 5.32 (m, 1H), 4.20−3.88 (m, 6H), 3.50 (m, 1H), 2.81 (m, 1H), 2.10−1.90 (m, 2H).

[(3a*S*,5*R*,7a*R*)-Hexahydro-2*H*-furo[2,3-*b*]pyran-5-yl] (4-Nitrophenyl) Carbonate (31g). The title compound was obtained from **30** as described for (−)-**7** in 70% yield. Purification and separation from the 5-*epi* diastereoisomer were performed following flash column chromatography on silica gel using hexanes/EtOAc (3:1, 2:1, then 1:1) as the eluent. Amorphous solid (70% from a 5:1 mixture of diastereoisomers). TLC: R_f = 0.16 (hexanes/EtOAc = 2:1). ^{1}H NMR (C_6D_6, 800 MHz) δ 7.64 (d, J = 9.0 Hz, 2H), 6.69 (d, J = 9.0 Hz, 2H), 4.76 d, J = 3.6 Hz, 1H), 4.35 (m, 1H), 4.02 (dt, J = 3.8, 8.6 Hz, 1H), 3.94 (dt, J = 2.8, 13.0 Hz, 1H), 3.60 (q, J = 8.0 Hz, 1H), 3.12 (dd, J = 2.0, 13.0 Hz), 2.04 (m, 1H), 1.67 (dq, J = 3.1, 15.1 Hz, 1H), 1.50 (m, 1H), 1.46−1.38 (m, 2H). ^{13}C NMR (C_6D_6, 200 MHz) δ 154.9, 151.9, 145.2, 124.9, 121.2, 100.7, 72.0, 67.4, 63.8, 35.9, 27.9, 27.3.

(3a*S*,4*S*,7a*R*)-Hexahydro-2*H*-furo[2,3-*b*]pyran-4-yl-(2*S*,3*R*)-4-(*N*-isobutyl-4-methoxyphenyl sulfonamido)-3-hydroxy-1-phenylbutan-2-yl Carbamate (35a). . Sulfonamide isostere **32** (42 mg, 0.08 mmol) was dissolved in a 30% TFA solution in CH_2Cl_2 (3 mL), the solution was stirred at 23 °C for 2 h after which the solvent was evaporated under reduced pressure. The corresponding Boc-deprotected intermediate (0.08 mmol) was then diluted in dry acetonitrile (0.8 mL) at 0 °C under argon and Et_3N (0.3 mL, 0.2 mmol) was added. A solution of activated carbonate **31a** (18.6 mg, 0.06 mmol) in acetonitrile or THF (0.5 mL) was then added to the mixture. The reaction was stirred at 23 °C until completion was reached (2−3 days). The solution was then evaporated *in vacuo* and the resulting residue purified by flash chromatography on silica gel using hexanes/EtOAc (2:1 then 1:1) as the eluent to afford the inhibitor **35a** as a amorphous solid (19.8 mg, 55%). TLC R_f = 0.35 (hexanes/EtOAc = 1:1). ^{1}H NMR ($CDCl_3$, 300 MHz) δ 7.71 (d, J = 8.9 Hz, 2H), 7.33−7.17 (m, 5H), 6.97 (d, J = 8.9 Hz, 2H), 5.05−4.90 (m, 1H), 4.93 (d, J = 3.6 Hz, 1H), 4.84 (d, J = 8.4 Hz, 1H), 4.15 (dt, J = 2.4, 9.0 Hz, 1H), 3.87 (s, 3H), 3.98−3.76 (m, 4H), 3.31 (t, J = 11.7 Hz, 1H), 3.22−2.90 (m, 4H), 2.90−2.78 (m, 2H), 2.48−2.32 (m, 1H), 1.96−1.25 (m, 5H), 0.92 (d, J = 6.6 Hz, 3H), 0.87 (d, J = 6.6 Hz, 3H). ^{13}C NMR ($CDCl_3$, 75 MHz) δ 163.1, 155.5, 137.6, 129.8, 129.4, 128.4, 126.5, 114.3, 101.1, 72.9, 70.2, 68.5, 60.9, 58.9, 55.7, 54.9, 53.8, 43.5, 35.6, 27.3, 26.2, 22.3, 20.2, 19.9. HRMS-ESI (m/z): [M + Na]$^+$ calcd for $C_{29}H_{40}N_2O_8NaS$ 599.2403, found 599.2406.

(3a*S*,4*S*,7a*R*)-Hexahydro-2*H*-furo[2,3-*b*]pyran-4-yl (2*S*,3*R*)-4-(4-Amino-*N*-isobutylphenylsulfonamido)-3-hydroxy-1-phenylbutan-2-yl Carbamate (36). The title compound was obtained from **31a** and sulfonamide isostere **33** as described for inhibitor **35a**, in 64% yield following purification by flash chromatography using $CHCl_3$/2% MeOH as the eluent. TLC: R_f = 0.45 (hexanes/EtOAc = 1:3). ^{1}H NMR ($CDCl_3$, 300 MHz) δ 7.55 (d, J = 8.7 Hz, 2H), 7.32−7.16 (m, 5H), 6.67 (d, J = 8.7 Hz, 2H), 4.97 (m, 1H), 4.93 (d, J = 3.4 Hz, 1H), 4.85 (d, J = 8.7 Hz, 1H), 4.20−4.11 (m, 3H), 3.92−3.80 (m, 5H), 3.31 (dt, J = 2.2, 11.9 Hz, 1H), 3.15 (dd, J = 8.1, 15.2 Hz, 1H), 3.05 (dd, J = 4.2, 14.1 Hz, 1H), 3.01−2.80 (m, 3H), 2.75 (dd, J = 6.6, 13.4 Hz, 1H), 2.40 (m, 1H), 1.97−1.60 (m, 4H), 1.46 (m, 1H), 0.92 (d, J = 6.6 Hz, 3H), 0.87 (d, J = 6.6 Hz, 3H). ^{13}C NMR ($CDCl_3$, 100 MHz) δ 155.5, 150.7, 137.7, 129.5, 129.5, 128.4, 126.5, 126.2, 114.1, 101.1, 72.8, 70.1, 68.5, 60.8, 58.9, 54.8, 53.8, 43.4, 35.5, 27.3, 26.2, 22.2, 20.2, 19.9. HRMS-ESI (m/z): [M + Na]$^+$ calcd for $C_{28}H_{39}N_3O_7NaS$ 584.2406; found 584.2402.

(3a*S*,4*S*,7a*R*)-Hexahydro-2*H*-furo[2,3-*b*]pyran-4-yl (2*S*,3*R*)-3-Hydroxy-4-(4-(hydroxymethyl)-*N*-isobutylphenylsulfonamido)-1-phenylbutan-2-yl Carbamate (37). The title compound was obtained from **31a** and sulfonamide isostere **34** as described for inhibitor **35a** in 72% yield following purification by flash chromatography on silica gel using $CHCl_3$/2% MeOH as the eluent. Amorphous solid. TLC: R_f = 0.23 (hexanes/EtOAc = 1:2). ^{1}H NMR ($CDCl_3$, 400 MHz) δ 7.76 (d, J = 8.1 Hz, 2H), 7.52 (d, J = 8.1 Hz, 2H), 7.32−7.17 (m, 5H), 4.96 (m, 1H), 4.93 (d, J = 3.2 Hz, 1H), 4.85 (d, J = 8.5 Hz, 1H), 4.80 (s, 2H), 4.15 (t, J = 8.5 Hz, 1H), 3.92−3.80 (m, 4H), 3.70 (s, 1H), 3.31 (t, J = 11.6 Hz, 1H), 3.16 (dd, J = 8.0, 15.0 Hz, 1H), 3.10−2.95 (m, 3H), 2.88−2.76 (m, 2H), 2.41 (m, 1H), 2.04 (m, 1H), 1.95−1.78 (m, 2H), 1.76−1.56 (m, 2H), 1.47 (m, 1H), 0.93 (d, J = 6.6 Hz, 3H), 0.88 (d, J = 6.6 Hz, 1H). ^{13}C NMR ($CDCl_3$, 100 MHz) δ 155.6, 146.2, 137.6, 137.1, 129.4 128.5, 127.6, 127.1, 126.5, 101.1, 72.8, 70.2, 68.4, 64.2, 60.8, 58.8, 54.9, 53.7, 43.4, 35.5, 27.3, 26.2, 22.2, 20.1, 19.9. HRMS-ESI (m/z): [M + Na]$^+$ calcd for $C_{29}H_{40}N_2O_8NaS$ 599.2403, found 599.2414.

(3a*R*,4*R*,7a*S*)-Hexahydro-2*H*-furo[2,3-*b*]pyran-4-yl ((2*S*,3*R*)-3-Hydroxy-4-(*N*-isobutyl-4-methoxyphenylsulfonamido)-1-phenylbutan-2-yl)carbamate (35b). The title compound was obtained from **31b** and sulfonamide isostere **32** in 65% yield as described for inhibitor **35a**, following purification by column chromatography on silica gel using hexanes/EtOAc (3:1, then 1.5:1) as the eluent. White amorphous solid. TLC: R_f = 0.44 (hexanes/EtOAc = 1:1). ^{1}H NMR ($CDCl_3$, 400 MHz) δ 7.70 (d, J = 8.9 Hz, 2H), 7.31−7.26 (m, 2H), 7.25−7.20 (m, 3H), 6.98 (d, J = 8.9 Hz, 2H), 5.00 (m, 1H), 4.97 (d, J = 2.7 Hz, 1H), 4.88 (d, J = 8.0 Hz, 1H), 4.17 (t, J = 7.7 Hz, 1H), 3.99−3.72 (m, 6H), 3.87 (s, 3H), 3.31 (dt, J = 1.9, 12.0 Hz, 1H), 3.13 (dd, J = 8.4, 15.0 Hz, 1H), 3.08−2.84 (m, 4H), 2.79 (dd, J = 6.7, 13.4 Hz, 1H), 2.53 (m, 1H), 2.00 (m, 1H), 1.83 (m, 1H), 1.73

(m, 1H), 1.68−1.54 (m, 2H). ^{13}C NMR ($CDCl_3$, 100 MHz) δ 163.1, 155.7, 137.7, 129.8, 129.5, 128.5, 126.5, 114.3, 101.2, 72.6, 70.2, 68.4, 60.8, 58.7, 55.6, 55.1, 53.7, 43.6, 35.3, 27.3, 26.2, 22.5, 20.1, 19.9. HRMS-ESI (*m/z*): $[M + Na]^+$ calcd for $C_{29}H_{40}N_2O_8NaS$ 599.2403, found 599.2407.

(3a*R*,4*S*,7a*R*)-Octahydrobenzofuran-4-yl (2*S*,3*R*)-3-Hydroxy-4-(*N*-isobutyl-4-methoxyphenylsulfonamido)-1-phenylbutan-2-yl Carbamate (35c). The title compound was obtained from **31c** and sulfonamide isostere **32** in 75% yield as described for inhibitor **35a**, following purification by column chromatography on silica gel using hexanes/EtOAc (3:1, then 2.5:1) as the eluent. TLC: R_f = 0.39 (hexanes/EtOAc = 1:1). ^{1}H NMR ($CDCl_3$, 400 MHz) δ 7.72 (d, J = 8.9 Hz, 2H), 7.311−7.16 (m, 5H), 6.98 (d, J = 8.9 Hz, 2H), 4.83 (m, 2H), 3.95−3.75 (m, 5H), 3.87 (s, 3H), 3.68 (q, J = 8.1 Hz, 1H), 3.14 (dd, J = 8.4, 15.2 Hz, 1H), 3.08 (dd, J = 4.1, 14.1 Hz, 1H), 3.05−2.99 (m, 1H), 2.96 (dd, J = 8.4, 13.4 Hz, 1H), 2.87−2.75 (m, 2H), 2.35 (m, 1H), 1.83 (m, 1H), 1.70−1.40 (m, 7H), 1.20 (m, 1H), 0.92 (d, J = 6.6 Hz, 3H), 0.87 (d, J = 6.6 Hz, 3H). ^{13}C NMR ($CDCl_3$, 100 MHz) δ 163.0, 156.1, 137.7, 129.7, 129.5, 129.4, 128.4, 126.4, 114.3, 73.0, 71.8, 66.6, 58.8, 55.6, 54.7, 53.7, 41.2, 35.6, 27.3, 27.2, 27.0, 25.7, 20.1, 19.9, 17.7. HRMS-ESI (*m/z*): $[M + Na]^+$ calcd for $C_{30}H_{42}N_2O_7NaS$ 597.2610, found 597.2621.

(4*S*,4a*R*,7a*S*)-Octahydrocyclopenta[*b*]pyran-4-yl ((2*S*,3*R*)-3-Hydroxy-4-(*N*-isobutyl-4-methoxyphenylsulfonamido)-1-phenylbutan-2-yl)carbamate (35d). The title compound was obtained from **31d** and sulfonamide isostere **32** in 81% yield as described for inhibitor **35a**, following purification by column chromatography on silica gel using hexanes/EtOAc (3:1, then 2.5:1) as the eluent. TLC: R_f = 0.58 (hexanes/EtOAc = 1:1). ^{1}H NMR ($CDCl_3$, 400 MHz) δ 7.70 (d, J = 8.9 Hz, 2H), 7.30−7.17 (m, 5H), 6.96 (d, J = 8.9 Hz, 2H), 4.94 (m, 1H), 4.81 (d, J = 8.1 Hz, 1H), 3.86 (s, 3H), 3.90−3.76 (m, 4H), 3.33 (t, J = 11.9 Hz, 1H), 3.13 (dd, AB, J = 8.3, 15.0 Hz, 1H), 3.08−2.91 (m, 3H), 2.85 (m, 1H), 2.79 (dd, J = 6.8, 13.5 Hz, 1H), 2.04 (m, 1H), 1.81 (m, 2H), 1.76−1.64 (m, 3H), 1.64−1.49 (m, 3H), 0.90 (d, J = 6.6 Hz, 3H), 0.86 (d, J = 6.6 Hz, 3H). ^{13}C NMR ($CDCl_3$, 100 MHz) δ 163.0, 156.0, 137.7, 129.8, 129.4, 128.4, 126.4, 114.3, 80.5, 72.7, 71.7, 65.2, 58.7, 55.6, 54.8, 53.7, 44.1, 35.6, 32.5, 27.2, 26.6, 22.0, 21.6, 20.1, 19.8. HRMS-ESI (*m/z*): $[M + Na]^+$ calcd for $C_{30}H_{42}N_2O_7S$ 597.2610, found 597.2612.

(3a*R*,4*S*,7a*R*)-Octahydro-1*H*-inden-4-yl-(2*S*,3*R*)-3-hydroxy-4-(*N*-isobutyl-4-methoxyphenylsulfonamido)-1-phenylbutan-2-yl Carbamate (35e). The title compound was obtained from **31e** and sulfonamide isostere **32** as described for inhibitor **35a**. Following preliminary purification by flash chromatography using hexanes/CH_2Cl_2/THF (8:1:1) as the eluent, the inhibitor was obtained as a mixture of unseparable isomeric compounds. Compound **35e** was derivatized into the corresponding *N,O*-isopropylidene compound by treatment of **35e** (20 mg) with 2,2-dimethoxypropane (0.1 mL) and a catalytic amount of *p*TSA (1.5 mg) in dry CH_2Cl_2 (1 mL) for 8 h at 23 °C. After neutralization with Et_3N, the organic phase was evaporated to dryness. Following a quick silica gel column (hexanes/EtOAc = 8:1), the resulting inhibitor was purified by HPLC: preparative HPLC column Sunfire Prep C18 OBD, 30 mm × 100 mm, eluent MeOH/H_2O 85:15 (30 min) and then 90:10 (15 min), flow rate 15 mL·min^{-1}, t_R = 42 min. The isopropylidene derivative was then obtained as a colorless oil (24 mg). The product was then taken into MeOH (2 mL). *p*TSA·H_2O (36 μmol, 1.5 mg) was added, and the resulting solution was refluxed for 6 h. After neutralization with a few drops of Et_3N, the solution was evaporated and the residue purified by column chromatography on silica gel using hexanes/CH_2Cl_2/THF (8:1:1) to give inhibitor **35e** (15 mg, 43% from **31e**). TLC: R_f = 0.35 (hexanes//EtOAc = 5:1). ^{1}H NMR ($CDCl_3$, 400 MHz) δ 7.71 (d, J = 8.9 Hz, 2H), 7.32−7.18 (m, 5H), 6.97 (d, J = 8.9 Hz, 2H), 4.79 (m, 1H), 4.70 (d. J = 8.1 Hz, 1H), 3.90 (m, 1H), 3.87 (s, 3H), 3.81 (m, 1H), 3.18−3.02 (m, 3H), 2.98−2.82 (m, 2H), 2.78 (dd, J = 6.6, 13.2 Hz, 1H), 2.10 (m, 1H), 1.90 (m, 1H), 1.82 (m, 1H), 1.74−1.19 (m, 11H), 0.95 (m, 1H), 0.90 (d, J = 6.6 Hz, 3H), 0.86 (d, J = 6.6 Hz, 3H). ^{13}C NMR ($CDCl_3$, 100 MHz) δ 163.0, 156.4, 137.7, 129.9, 129.5, 129.4, 128.5, 126.4, 114.3, 74.9, 72.8, 58.8, 55.6, 54.8, 53.8, 43.1, 39.9, 35.7, 31.3, 27.2, 26.9, 26.1, 23.5, 22.2, 21.3, 20.1, 19.9. HRMS-ESI (*m/z*): $[M + Na]^+$ calcd for $C_{31}H_{44}N_2O_6NaS$ 595.2818, found 595.2816.

(4*S*,4a*S*,7a*R*)-Hexahydro-2*H*-furo[3,4-*b*]pyran-4-yl ((2*S*,3*R*)-3-Hydroxy-4-(*N*-isobutyl-4-methoxyphenylsulfonamido)-1-phenylbutan-2-yl)carbamate (35f). The title compound was obtained from **31f** and sulfonamide isostere **32** in 75% yield as described for inhibitor **35a**, following purification by column chromatography using hexanes/EtOAc (3:1, then 2.5:1) as the eluent. TLC: R_f = 0.24 (hexanes/EtOAc = 1:1). ^{1}H NMR ($CDCl_3$, 800 MHz) δ 7.70 (d, J = 8.8 Hz, 2H), 7.30 (m, 2H), 7.24−7.20 (m, 3H), 6.97 (d, J = 8.8 Hz, 2H), 5.05 (m, 1H), 4.83 (d, J = 8.5 Hz, 1H), 4.03 (t, J = 3.2 Hz, 1H), 3.96 (m, 1H), 3.87 (s, 3H), 3.87 (s, 3H), 3.88−3.81 (m, 5H), 3.62 (t, J = 8.3 Hz, 1H), 3.39 (t, J = 11.5 Hz, 1H), 3.14 (dd, J = 8.4, 15.0 Hz, 1H), 3.02 (dd, J = 4.0, 14.1 Hz, 1H), 2.99−2.94 (m, 2H), 2.84 (dd, J = 8.7, 14.1 Hz, 1H), 2.77 (dd, J = 6.6, 13.4 Hz, 1H), 2.51 (m, 1H), 1.81 (m, 1H), 1.78 (dq, J = 4.5, 12.4 Hz, 1H), 1.71 (dd, J = 5.4, 12.4 Hz, 1H), 0.91 (d J = 6.6 Hz, 3H), 0.87 (d, J = 6.6 Hz, 3H). ^{13}C NMR ($CDCl_3$, 200 MHz) δ 163.0, 155.5, 137.5, 129.6, 129.45, 129.38, 128.5, 126.6, 114.3, 78.4, 74.4, 72.6, 70.0, 66.1, 64.9, 58.8, 55.6, 54.9, 53.7, 42.7, 35.4, 27.2, 26.9, 20.1, 19.8. HRMS-ESI (*m/z*): $[M + Na]^+$ calcd for $C_{29}H_{40}N_2O_8S$ 599.2403, found 599.2397.

(3a*S*,5*R*,7a*R*)-Hexahydro-2*H*-furo[2,3-*b*]pyran-5-yl ((2*S*,3*R*)-3-Hydroxy-4-(*N*-isobutyl-4-methoxyphenylsulfonamido)-1-phenylbutan-2-yl)carbamate (35g). The title compound was obtained from **31g** and sulfonamide isostere **32** in 86% yield as described for inhibitor **35a**, following purification by column chromatography on silica gel using hexanes/EtOAc (gradient 3:1 to 1.5:1) as the eluent. TLC: R_f = 0.33 (hexanes/EtOAc = 1:1). ^{1}H NMR ($CDCl_3$, 400 MHz) δ 7.72 (d, J = 8.9 Hz, 2H), 7.32−7.26 (m, 2H), 7.25−7.17 (m, 3H), 6.98 (d, J = 8.9 Hz, 2H), 4.98 (d, J = 3.5 Hz, 1H), 4.89 (d, J = 8.7 Hz, 1H), 4.54 (m, 1H), 4.11 (dt, J = 3.5, 8.3 Hz, 1H), 3.87 (s, 3H), 3.90−3.77 (m, 4H), 3.74 (m, 1H), 3.56 (d, J = 12.7 Hz, 1H), 3.12 (dd, J = 8.5, 15.1 Hz, 1H), 3.09−2.91 (m, 3H), 2.84 (dd, J = 8.5, 14.1 Hz, 1H), 2.79 (dd, J = 6.8, 13.4 Hz, 1H), 2.08 (m, 1H), 2.04−1.93 (m, 2H), 1.90−1.76 (m, 3H), 0.91 (d, J = 6.6 Hz, 3H), 0.87 (d, J = 6.6 Hz, 3H). ^{13}C NMR ($CDCl_3$, 100 MHz) δ 163.4, 155.7, 137.6, 129.7, 129.5, 128.5, 126.5, 114.4, 101.0, 72.5, 68.0, 67.1, 65.4, 58.8, 55.6, 54.9, 53.8, 36.2, 35.8, 28.3, 27.8, 27.2, 20.1, 19.9. HRMS-ESI (*m/z*): $[M + Na]^+$ calcd for $C_{29}H_{40}N_2O_8NaS$ 599.2403, found 599.2397.

Acknowledgment. The research was supported by the National Institutes of Health (Grant GM53386). This work was also supported by the Intramural Research Program of the Center for Cancer Research, National Cancer Institute, National Institutes of Health, and in part by a Grant-in-Aid for Scientific Research (Priority Areas) from the Ministry of Education, Culture, Sports, Science, and Technology of Japan (Monbu Kagakusho), a Grant for Promotion of AIDS Research from the Ministry of Health, Welfare, and Labor of Japan (Kosei Rohdosho), and a Grant to the Cooperative Research Project on Clinical and Epidemiological Studies of Emerging and Reemerging Infectious Diseases (Renkei Jigyo) of Monbu-Kagakusho.

Supporting Information Available: HPLC and HRMS data of inhibitors **35a−g**, **36**, and **37**. This material is available free of charge via the Internet at http://pubs.acs.org.

References

(1) Conway, B. HAART in Treatment-Experienced Patients in the 21st Century: The Audacity of Hope. *Future Virol.* **2009**, *4*, 39–41.
(2) Bartlett, J. A.; DeMasi, R.; Quinn, J.; Moxham, C.; Rousseau, F. Overview on the Effectiveness of Triple Combination Therapy in

Antiretroviral-Naive HIV-1 Infected Adults. *AIDS* **2001**, *15*, 1369–1377.
(3) Walensky, R. P.; Paltiel, A. D.; Losina, E.; Mercincavage, L. M.; Schackman, B. R.; Sax, P. E.; Weinstein, M. C.; Freedberg, K. A. The Survival Benefits of AIDS Treatment in the United States. *J. Infect. Dis.* **2006**, *194*, 11–19.
(4) Sepkowitz, K. A. AIDS: The First 20 Years. *N. Engl. J. Med.* **2001**, *344*, 1764–1772.
(5) Palella, F. J., Jr.; Delaney, K. M.; Moorman, A. C.; Loveless, M. O.; Fuhrer, J.; Satten, G. A.; Aschman, D. J.; Holmberg, S. D. Declining Morbidity and Mortality among Patients with Advanced Human Immunodeficiency Virus Infection. *N. Engl. J. Med.* **1998**, *338*, 853–860.
(6) De Clercq, E. Anti-HIV Drugs: 25 Compounds Approved within 25 Years after the Discovery of HIV. *Int. J. Antimicrob. Agents* **2009**, 307–320.
(7) Pillay, D.; Bhaskaran, K.; Jurriaans, S.; Prins, M.; Masquelier, B.; Dabis, F.; Gifford, R.; Nielsen, C.; Pedersen, C.; Balotta, C.; Rezza, G.; Ortiz, M.; de Mendoza, C.; Kucherer, C.; Poggensee, G.; Gill, J.; Porter, K. The Impact of Transmitted Drug Resistance on the Natural History of HIV Infection and Response to First-Line Therapy. *AIDS* **2006**, *20*, 21–28.
(8) Grabar, S.; Pradier, C.; Le Corfec, E.; Lancar, R.; Allavena, C.; Bentata, M.; Berlureau, P.; Dupont, C.; Fabbro-Peray, P.; Poizot-Martin, I.; Costagliola, D. Factors Associated with Clinical and Virological Failure in Patients Receiving a Triple Therapy Including a Protease Inhibitor. *AIDS* **2000**, *14*, 141–149.
(9) Little, S. J.; Holte, S.; Routy, J. P.; Daar, E. S.; Markowitz, M.; Collier, A. C.; Koup, R. A.; Mellors, J. W.; Connick, E.; Conway, B.; Kilby, M.; Wang, L.; Whitcomb, J. M.; Hellmann, N. S.; Richman, D. D. Antiretroviral-Drug Resistance among Patients Recently Infected with HIV. *N. Engl. J. Med.* **2002**, *347*, 385–394.
(10) Grant, R. M.; Hecht, F. M.; Warmerdam, M.; Liu, L.; Liegler, T.; Petropoulos, C. J.; Hellmann, N. S.; Chesney, M.; Busch, M. P.; Kahn, J. O. Time Trends in Primary HIV-1 Drug Resistance among Recently Infected Persons. *JAMA, J. Am. Med. Assoc.* **2002**, *288*, 181–188.
(11) Hue, S.; Gifford, R. J.; Dunn, D.; Fernhill, E.; Pillay, D. On behalf of the UK Collaborative Group on HIV Drug Resistance. Demonstration of Sustained Drug-Resistant Human Immunodeficiency Virus Type 1 Lineages Circulating among Treatment-Naive Individuals. *J. Virol.* **2009**, *83*, 2645–2654.
(12) Lucas, G. M. Antiretroviral Adherence, Drug Resistance, Viral Fitness and HIV Disease Progression: A Tangled Web Is Woven. *J. Antimicrob. Chemother.* **2005**, *55*, 413–416.
(13) Spaltenstein, A.; Kazmierski, W. M.; Miller, J. F.; Samano, V. Discovery of Next Generation Inhibitors of HIV Protease. *Curr. Top. Med. Chem.* **2005**, *5*, 1589–1607.
(14) Ghosh, A. K.; Sridhar, P. R.; Kumaragurubaran, N.; Koh, Y.; Weber, I. T.; Mitsuya, H. Bis-tetrahydrofuran: A Privileged Ligand for Darunavir and a New Generation of HIV-Protease Inhibitors That Combat Drug-Resistance. *ChemMedChem* **2006**, *1*, 939–950.
(15) Ghosh, A. K.; Sridhar, P. R.; Leshchenko, S.; Hussain, A. K.; Li, J.; Kovalevsky, A. Yu.; Walters, D. E.; Wedekind, J. E.; Grum-Tokars, V.; Das, D.; Koh, Y.; Maeda, K.; Gatanaga, H.; Weber, I. T.; Mitsuya, H. Structure-Based Design of Novel HIV-1 Protease Inhibitors To Combat Drug Resistance. *J. Med. Chem.* **2006**, *49*, 5252–5261.
(16) Ghosh, A. K.; Xu, C.-X.; Rao, K. V.; Baldridge, A.; Agniswamy, J.; Wang, Y.-F.; Weber, I. T.; Aoki, M.; Miguel, S. G. P.; Amano, M.; Mitsuya, H. Probing Multidrug-Resistance/Protein−Ligand Interaction with New Oxatricyclic Designed Ligands in HIV-1 Protease Inhibitors. *ChemMedChem* **2010**, *5*, 1850–1854.
(17) FDA News Release, June 23, 2006: FDA Approves New HIV Treatment for Patients Who Do Not Respond to Existing Drugs. http://www.fda.gov/NewsEvents/Newsroom/PressAnnouncements/2006/ucm108676.htm.
(18) On October 21, 2008, FDA expanded approval to Prezista (darunavir), coadministered with ritonavir and with other antiretroviral agents, for the treatment of HIV-1 infection in treatment-naive adult patients. In addition to the traditional approval, a new dosing regimen for treatment-naive adult patients was approved.
(19) Koh, Y.; Nakata, H.; Maeda, K.; Ogata, H.; Bilcer, G.; Devasamudram, T.; Kincaid, J. F.; Boross, P.; Wang, Y.-F.; Tie, Y.; Volarath, P.; Gaddis, L.; Harrison, R. W.; Weber, I. T.; Ghosh, A. K.; Mitsuya, H. Novel Bis-tetrahydrofuranylurethane-Containing Nonpeptidic Protease Inhibitor (PI) UIC-94017 (TMC114) with Potent Activity against Multi-PI-Resistant Human Immunodeficiency Virus in Vitro. *Antimicrob. Agents Chemother.* **2003**, *47*, 3123–3129.
(20) De Meyer, S.; Azijn, H.; Surleraux, D.; Jochmans, D.; Tahri, A.; Pauwels, R.; Wigerinck, P.; de Bethune, M.-P. TMC114, a Novel Human Immunodeficiency Virus Type 1 Protease Inhibitor Active against Protease Inhibitor-Resistant Viruses, Including a Broad Range of Clinical Isolates. *Antimicrob. Agents Chemother.* **2005**, *49*, 2314–2321.
(21) Lefebvre, E.; Schiffer, C. A. Resilience to Resistance of HIV-1 Protease Inhibitors: Profile of Darunavir. *AIDS Rev.* **2008**, *10*, 131–142.
(22) Ghosh, A. K.; Chapsal, B. D.; Weber, I. T.; Mitsuya, H. Design of HIV Protease Inhibitors Targeting Protein Backbone: An Effective Strategy for Combating Drug Resistance. *Acc. Chem. Res.* **2008**, *41*, 78–86.
(23) Tie, Y.; Boross, P. I.; Wang, Y.-F.; Gaddis, L.; Hussain, A. K.; Leshchenko, S.; Ghosh, A. K.; Louis, J. M.; Harrison, R. W.; Weber, I. T. High Resolution Crystal Structures of HIV-1 Protease with a Potent Non-Peptide Inhibitor (UIC-94017) Active against Multi-Drug-Resistant Clinical Strains. *J. Mol. Biol.* **2004**, *338*, 341–352.
(24) King, N. M.; Prabu-Jeyabalan, M.; Nalivaika, E. A.; Wigerinck, P.; de Bethune, M.-P.; Schiffer, C. A. Structural and Thermodynamic Basis for the Binding of TMC114 a Next-Generation Human Immunodeficiency Virus Type 1 Protease Inhibitor. *J. Virol.* **2004**, *78*, 12012–12021.
(25) Kovalevsky, A. Y.; Liu, F.; Leshchenko, S.; Ghosh, A. K.; Louis, J. M.; Harrison, R. W.; Weber, I. T. Ultra-High Resolution Crystal Structure of HIV-1 Protease Mutant Reveals Two Binding Sites for Clinical Inhibitor TMC114. *J. Mol. Biol.* **2006**, *363*, 161–173.
(26) Amano, M.; Koh, Y.; Das, D.; Li, J.; Leschenko, S.; Wang, Y.-F.; Boross, P. I.; Weber, I. T.; Ghosh, A. K.; Mitsuya, H. A Novel Bis-tetrahydrofuranylurethane-Containing Nonpeptidic Protease Inhibitor (PI), GRL-98065, Is Potent against Multi-PI-Resistant Human Immunodeficiency Virus in Vitro. *Antimicrob. Agents Chemother.* **2007**, *51*, 2143–2155.
(27) (a) Nakashima, H.; Masayuki, S.; Taniguchi, T.; Ogasawara, K. Chiral Preparation of Polyoxygenated Cyclopentanoids. *Synthesis* **2000**, *6*, 817–823. (b) Laumen, K.; Schneider, M. P. A Facile Chemoenzymatic Route to Optically Pure Building Blocks for Cyclopentanoid Natural Products. *J. Chem. Soc., Chem. Commun.* **1986**, 1298–1299.
(28) Ishihara, K.; Kurihara, H.; Yamamoto, H. An Extremely Simple, Convenient, and Selective Method for Acylating Primary Alcohols in the Presence of Secondary Alcohols. *J. Org. Chem.* **1993**, *58*, 3791–3793.
(29) Nara, M.; Terashima, S.; Yamada, S. Stereochemical Studies—LVII Synthesis of Optically Active Compounds by the Novel Use of Meso-Compounds—1. Efficient Synthesis of Two Structural Types of Optically Pure Prostaglandin Intermediates. *Tetrahedron* **1980**, *36*, 3161–3170.
(30) Moriarty, R. M.; Bailey, B. R., III.; Prakash, O.; Prakash, I. Capture of Electron-Deficient Species with Aryl Halides. New Syntheses of Hypervalent Iodonium Ylides. *J. Am. Chem. Soc.* **1985**, *107*, 1375–1378.
(31) Müller, P.; Allenbach, Y. F.; Bernardinelli, G. On the Enantioselectivity of Transition Metal-Catalyzed 1,3-Cycloadditions of 2-Diazocyclohexane-1,3-diones. *Helv. Chim. Acta* **2003**, *86*, 3164–3178.
(32) Ferrie, L.; Reymond, S.; Capdevielle, P.; Cossy, J. Formal Chemoselective Synthesis of Leucascandrolide A. *Org. Lett.* **2007**, *9*, 2461–2464.
(33) Tsantali, G. G.; Takakis, I. M. Expeditious Copper-Catalyzed Conjugate 1,4-Addition of Bromo[2-(1,3-dioxolan-2-yl)ethyl]magnesium to α,β-Cycloalkenones and Subsequent Tranformations. *J. Org. Chem.* **2003**, *68*, 6455–6458.
(34) Shen, Z.-L.; Geo, G.-L.; Loh, T.-P. Indium-Copper and Indium-Silver Mediated Barbier Grignard Type Alkylation Reaction of Aldehydes Using Unactivated Alkyl Halides in Water. *J. Org. Chem.* **2008**, *73*, 3922–3924.
(35) Ghosh, A. K.; Leschenko, S.; Noetzel, M. Stereoselective Photochemical 1,3-Dioxolane Addition to 5-Alkoxymethyl-2(5*H*)-furanone: Synthesis of Bis-tetrahydrofuranyl Ligand for HIV Protease Inhibitor UIC-94017 (TMC-114). *J. Org. Chem.* **2004**, *69*, 7822–7829.
(36) Toth, M. V.; Marshall, G. R. A Simple Continuous Fluorometric Assay for HIV Protease. *Int. J. Pept. Protein Res.* **1990**, *36*, 544–550.
(37) Halgren, T. A. MMFF VII. Characterization of MMFF94, MMFF94s, and Other Widely Available Force Fields for Conformational Energies and for Intermolecular-Interaction Energies and Geometries. *J. Comput. Chem.* **1999**, *20*, 730–748.
(38) Hodgson, D. M.; Lee, G. P.; Marriot, R. E.; Thompson, A. J.; Wisedale, R.; Witherington, J. Isomerisations of Cycloalkene- and Bicycloalkene-Derived Achiral Epoxides by Enantioselective α-Deprotonation. *J. Chem. Soc., Perkin Trans. 1* **1998**, 2151–2161.

CHEMMEDCHEM

DOI: 10.1002/cmdc.201000318

Probing Multidrug-Resistance and Protein–Ligand Interactions with Oxatricyclic Designed Ligands in HIV-1 Protease Inhibitors

Arun K. Ghosh,*[a] Chun-Xiao Xu,[a] Kalapala Venkateswara Rao,[a] Abigail Baldridge,[a] Johnson Agniswamy,[b] Yuan-Fang Wang,[b] Irene T. Weber,[b] Manabu Aoki,[c] Salcedo Gomez Pedro Miguel,[c] Masayuki Amano,[c] and Hiroaki Mitsuya[c, d]

The introduction of HIV-1 protease inhibitors (PIs) into highly active antiretroviral therapy (HAART) in 1996 had a critical impact in decreasing HIV-related morbidity and mortality.[1] Indeed, HAART regimens with PIs initially suppressed HIV-1 replication in patients to undetectable HIV-1 RNA levels in plasma.[2] However, one of the serious shortcomings of current treatments is the rapid emergence of drug-resistant HIV strains.[3] There is an urgent need for improved PIs for the treatment of the increasing number of treatment-experienced patients harboring multidrug-resistant HIV-1 strains.[4,5]

We recently reported a number of PIs that were developed by incorporating structure-based designed novel nonpeptide ligands/scaffolds that target the HIV-1 protease substrate binding site.[6–17] One of the PIs, darunavir (**1**, DRV, Figure 1), was first approved for HIV/AIDS patients harboring drug-resistant HIV who do not respond to other antiretroviral drugs.[11] Recently, DRV has received full approval for all HIV/AIDS patients, including children infected with HIV-1.[12] DRV has a stereochemically defined fused *bis*-tetrahydrofuran (*bis*-THF) moiety as the P2 ligand.[7,8] The X-ray crystal structures of the complexes of both **1**- and **2**-bound HIV-1 protease revealed extensive protein–ligand hydrogen bonding interactions involving the backbone of HIV-1 protease throughout the active site.[13,14] In particular, both oxygen atoms of the P2 *bis*-THF ligand are involved in hydrogen bonding with Asp29 and Asp30 backbone NH groups.[15] In addition, the bicyclic ligand appears to fill the hydrophobic pocket at the S2 subsite. The P2 *bis*-THF ligand is responsible for the superior drug-resistance properties of both DRV (**1**) and TMC-126 (**2**). In our preliminary investigation, we chose to incorporate *para*-methoxysulfonamide as the P2′ ligand owing to its marked hydrogen bonding interaction in the S2′ site. To combat drug resistance, our inhibitor design strategies focused on maximizing inhibitor interactions with

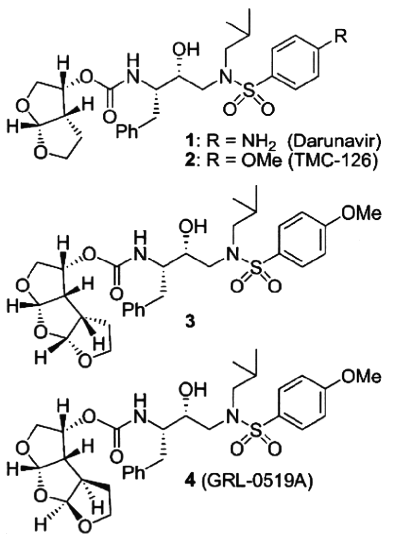

Figure 1. Structure of darunavir (DRV, **1**) and protease inhibitors **2–4**.

the HIV-1 protease active site, particularly by promoting extensive hydrogen bond interactions with the protein backbone atoms.[15] We have recently shown that the enhancement of 'backbone binding' leads to the design of PIs that maintain full potency against a panel of multidrug-resistant HIV-1 variants.[17] Based on our examination of the protein–ligand crystal structure of DRV-bound HIV-1 protease, we have further speculated that the incorporation of another tetrahydrofuran ring on the *bis*-THF ligand would provide additional ligand–binding site interactions. Particularly, it appears that the ligand oxygen atoms can effectively maintain backbone hydrogen bonding with Asp29 and Asp30, and can fill the hydrophobic pocket effectively. This in turn could further improve drug-resistance properties of the PIs. Such oxatricyclic ligands could have a variety of possible stereochemical motifs, including *syn-syn-syn* (*SSS*-type) and *syn-anti-syn* (*SAS*-type) isomers. Our X-ray crystal structure-based preliminary modeling suggested that the *SAS*-type ligand-based inhibitor **4** would make enhanced interactions in the S2 subsite relative to the *SSS*-derived inhibitor **3** (Figure 1).

The synthesis of the oxatricyclic *tris*-THF ligand with an *SSS* configuration was carried out as shown in Scheme 1. Optically active *bis*-THF derivatives **6** and **7** were conveniently prepared in multi-gram quantities from dihydrofuran **5** in a three-step sequence followed by lipase-catalyzed optical resolution as described previously.[18,19] Optically active alcohol **7** was treated with triphenylphosphine and iodine in the presence of imidazole to provide the corresponding iodide. Treatment of the re-

[a] *Prof. Dr. A. K. Ghosh, Dr. C.-X. Xu, Dr. K. V. Rao, A. Baldridge*
Department of Chemistry and Medicinal Chemistry
Purdue University, 560 Oval Drive, West Lafayette, IN 47907 (USA)
Fax: (+1) 765-496-1612
E-mail: akghosh@purdue.edu

[b] *J. Agniswamy, Y.-F. Wang, Prof. Dr. I. T. Weber*
Department of Biology, Molecular Basis of Disease
Georgia State University, Atlanta, GA 30303 (USA)

[c] *M. Aoki, S. G. P. Miguel, M. Amano, Dr. H. Mitsuya*
Departments of Hematology and Infectious Diseases
Kumamoto University School of Medicine, Kumamoto 860-8556 (Japan)

[d] *Dr. H. Mitsuya*
Experimental Retrovirology Section, HIV and AIDS Malignancy Branch
National Cancer Institute, Bethesda, MD 20892 (USA)

Supporting information for this article is available on the WWW under http://dx.doi.org/10.1002/cmdc.201000318.

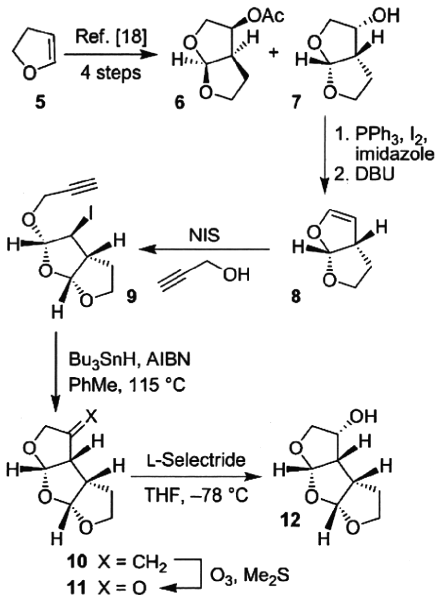

Scheme 1. Synthesis of the *syn-syn-syn tris*-THF ligand **12**.

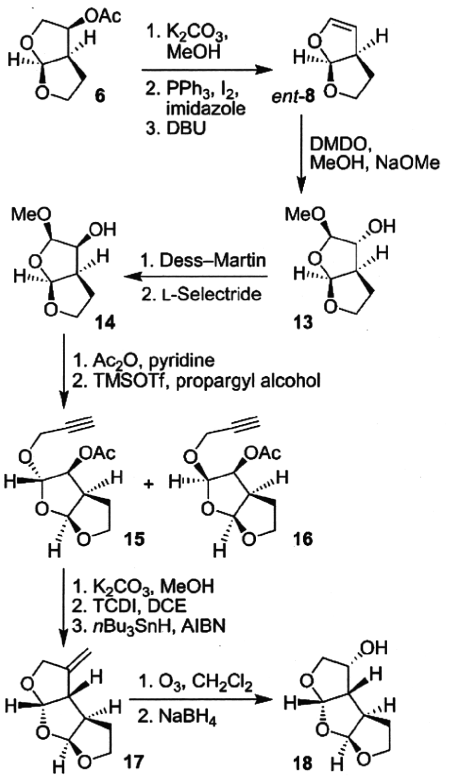

Scheme 2. Synthesis of the *syn-anti-syn tris*-THF alcohol **18**.

sulting iodide with 1,8-diazabicyclo[5.4.0]undec-7-ene (DBU) furnished volatile bicyclic enol ether **8**. Reaction of **8** with *N*-iodosuccinimide (NIS) and propargyl alcohol in dichloromethane at 0–23 °C afforded iodoether **9** in 58% yield over three steps.[18] Radical cyclization of **9** with tri(*n*-butyl)tin hydride in the presence of azobisisobutyronitrile (AIBN) in toluene at reflux provided tricyclic olefin **10**. The relative stereochemistry of the tricyclic core was established by extensive NMR experiments (COSY, NOESY). Ozonolysis of the olefin, followed by L-selectride reduction of the resulting ketone furnished *endo*-alcohol **12** as a single isomer (by ^{1}H NMR analysis).

The synthesis of *tris*-THF ligand with a *SAS* ring fused system is shown in Scheme 2. Optically active (3*S*,3a*R*,6a*S*)-*bis*-THF alcohol *ent*-**7** was readily obtained by saponification of acetate derivative **6**. It was converted into bicyclic enol ether *ent*-**8** as described above. This enol ether was exposed to acetone-free dimethyldioxirane (DMDO)[20] in dichloromethane at −78 °C to provide the corresponding epoxide. Treatment of the resulting epoxide with a catalytic amount of sodium methoxide (10%) in methanol provided epoxide-opened product **13** as a single diastereomer.[21] The depicted stereochemistry of **13** was fully supported by extensive NMR studies. Dess–Martin oxidation[22] of **13** followed by L-selectride reduction of the resulting ketone provided *endo*-alcohol **14** as a single isomer in 68% yield over two steps. To append the third oxacyclic ring, alcohol **14** was first acylated, and the resulting acetate was treated with trimethylsilyl trifluoromethanesulfonate (TMSOTf) and propargyl alcohol, which afforded acetals **15** and **16** as a 4:1 mixture of diastereomers. The isomers could not be separated at this stage; however, removal of the acetate provided the corresponding alcohols, which were readily separated by column chromatography. The major diastereomeric alcohol was converted into tricyclic olefin **17** in a two-step sequence involving: 1) reaction of alcohol with thiocarbonyldiimidazole (TCDI) in dichloroethane (DCE) to provide the corresponding thiocarbamate, and 2) treatment of the resulting thiocarbamate with tri(*n*-butyl)tin hydride in the presence of AIBN in toluene at reflux to provide olefin **17** in 75% yield over two steps.[23] The stereochemistry of olefin **17** was established by ^{1}H NMR spectroscopy. Olefin **17** was converted into *endo*-alcohol **18** by ozonolysis of the olefin followed by sodium borohydride reduction of the resulting ketone to furnish **18** as a single isomer. Mosher ester analysis[24] revealed high optical purity (99% *ee*).

The synthesis of *tris*-THF-containing PIs is shown in Scheme 3. Optically active *tris*-THF ligand alcohols **12** and **18** were converted into the corresponding *para*-nitrophenyl carbonates **19** and **20** by treatment with *para*-nitrophenyl chloroformate and *N*-methylmorpholine (NMM). Treatment of amine **21**,[25] synthesized previously, with activated carbonate **19** or **20** in the presence of diisopropylethylamine (DIPEA) provided PIs **3** and **4** in 65% yield.

Inhibitor **3** shows potent inhibitory activity (K_i = 60 pM). In comparison, inhibitor **4** (GRL-0519A, Figure 1) has a K_i value of 5.9 pM, a 10-fold improvement over **3**. Both PIs **3** (IC_{50} = 3.5 nM) and **4** (IC_{50} = 1.8 nM) also showed excellent antiviral activity against the wild-type HIV-1_{LAI}. PI **4** (GRL-0519A) was the most potent against a laboratory HIV-1 strain, HIV-1_{LAI}, with an EC_{50} value of 1.8 nM and a favorable cytotoxicity profile (CC_{50} = 44.6 μM) as examined by using MT-2 cells as target cells, producing a selectivity index (CC_{50}/EC_{50}) of 24778.

We next examined GRL-0519A against a variety of primary HIV-1 strains, which were isolated from patients with AIDS who had failed a number of anti-HIV therapeutic regimens after re-

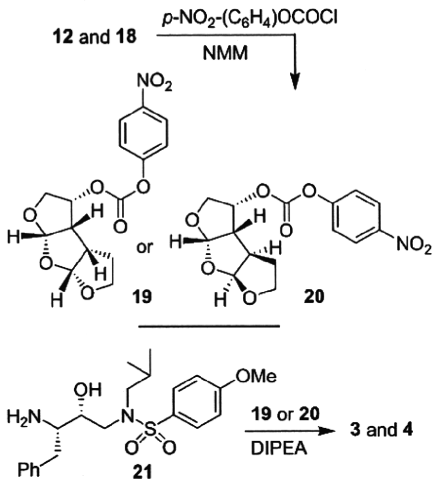

Scheme 3. Synthesis of inhibitors **3** and **4**.

ceiving 9–11 anti-HIV-1 drugs over the previous 32–83 months, and who proved to be highly resistant to multiple PIs.[9,26] These primary strains contain 9–14 amino acid substitutions in the protease-encoding region of the HIV-1 genome which have been reported to be associated with HIV-1 resistance against various PIs.[27] The substitutions identified include Leu10→Ile (L10I; 6 of 6 isolates), M46I/L (6 of 6), I54V (4 of 6), L63P (6 of 6), A71V/T (5 of 6), V82A (6 of 6), and L90M (4 of 6) (see the footnote of Table 1).

Darunavir (DRV) is more potent against wild-type HIV-$1_{ERS104pre}$ (EC_{50} = 0.005 μM) than amprenavir (APV),[28] which has an EC_{50} value of 0.032 μM. DRV was moderately less active against a panel of multidrug-resistant HIV-1 variants, with EC_{50} values ranging from 0.011 to 0.031 μM. The fold difference in EC_{50} values was 2–6 relative to its EC_{50} value against HIV-$1_{ERS104pre}$. APV was less active against the variants, with EC_{50} values and fold differences ranging between 0.291 and 0.521 μM, and from 9 to 16, respectively. GRL-0519A exerted the greatest potency among the three agents against wild-type HIV-$1_{ERS104pre}$, with an EC_{50} value of 0.6 nM. GRL-0519A was less potent against the variants, with EC_{50} values ranging from 0.9 to 4.3 nM, and the fold difference was 2–7 relative to wild-type HIV-1 (Table 1). Importantly, GRL-0519A is more potent than DRV by a factor of 5.9–14 in comparing absolute concentrations of EC_{50} values.

Dimerization of HIV-1 protease subunits is an essential process for the acquisition of proteolytic activity, which plays a critical role in the maturation and replication of the virus.[29] We previously demonstrated that a group of compounds, including DRV and TPV, inhibit the dimerization of HIV-1 protease monomer subunits as examined by a FRET-based HIV-1 expression assay that uses cyan (CFP) and yellow fluorescent protein (YFP)-tagged protease monomers; other conventional FDA-approved PIs such as APV failed to block dimerization.[30] As shown in Figure 2, the average $CFP^{A/B}$ ratio determined in the cells transfected and cultured in the absence of drug was 1.1 ± 0.13, indicating that protease dimerization efficiently occurred. In the same assay, in the presence of DRV at 0.1 and 1 μM, the average $CFP^{A/B}$ ratios determined were 0.93 ± 0.07 and 0.81 ± 0.11, respectively, indicating that DRV effectively inhibits protease dimerization at those concentrations. However, the average ratios were greater than 1.0 at 0.001 and 0.01 μM, indicating that no dimerization inhibition occurred at these lower DRV concentrations, in line with the data we previously reported.[30] We next examined whether GRL-0519A can block protease dimerization under exactly the same conditions in the FRET-based HIV-1 expression assay. When the ratios were determined in the cells transfected and cultured in the presence of GRL-0519A at 0.01, 0.1, and 1 μM, the average values were 0.96 ± 0.07, 0.84 ± 0.09, and 0.84 ± 0.11, respectively, indicating that GRL-0519A can block protease dimerization more potently, by at least 10-fold, relative to DRV.

Table 1. Antiviral activity of GRL-0519A (**4**), amprenavir (APV), and darunavir (DRV) against multidrug-resistant clinical isolates in PHA-PBMs.[a]

Virus	EC_{50} [μM] GRL-0519A	APV	DRV
HIV-$1_{ERS104pre}$ (wild-type: X4)	0.0006 ± 0.0002	0.032 ± 0.006	0.005 ± 0.002
HIV-$1M_{DR/B}$ (X4)	0.0043 ± 0.0012 (7)	0.521 ± 0.203 (16)	0.028 ± 0.008 (6)
HIV-$1M_{DR/C}$ (X4)	0.0009 ± 0.0002 (2)	0.357 ± 0.040 (11)	0.011 ± 0.004 (2)
HIV-$1M_{DR/G}$ (X4)	0.0027 ± 0.0012 (5)	0.485 ± 0.073 (15)	0.031 ± 0.002 (6)
HIV-$1M_{DR/TM}$ (X4)	0.0022 ± 0.0001 (4)	0.488 ± 0.009 (15)	0.031 ± 0.002 (6)
HIV-$1M_{DR/MM}$ (R5)	0.0027 ± 0.0006 (5)	0.291 ± 0.128 (9)	0.016 ± 0.006 (3)
HIV-$1M_{DR/JSL}$ (R5)	0.0028 ± 0.0001 (5)	0.419 ± 0.122 (13)	0.024 ± 0.007 (5)

[a] The amino acid substitutions identified in the protease-encoding region of HIV-$1_{ERS104pre}$, HIV-1_B, HIV-1_C, HIV-1_G, HIV-1_{TM}, HIV-$1M_M$, HIV-1_{JSL} compared with the consensus type B sequence cited from the Los Alamos database include L63P; L10I, K14R, L33I, M36I, M46I, F53I, K55R, I62V, L63P, A71V, G73S, V82A, L90M, I93L; L10I, I15V, K20R, L24I, M36I, M46L, I54V, I62V, L63P, K70Q, V82A, L89M; L10I, V11I, T12E, I15V, L19I, R41K, M46L, L63P, A71T, V82A, L90M; L10I, K14R, R41K, M46L, I54V, L63P, A71V, V82A, L90M, I93L; L10I, K43T, M46L, I54V, L63P, A71V, V82A, L90M, Q92K; and L10I, L24I, I33F, E35D, M36I, N37S, M46L, I54V, R57K, I62V, L63P, A71V, G73S, V82A, respectively. HIV-$1_{ERS104pre}$ served as a source of wild-type HIV-1. The EC_{50} values were determined by using PHA-PBMs as target cells, and the inhibition of p24 gag protein production by each drug was used as an endpoint. The numbers in parentheses represent the fold change in EC_{50} value for each isolate relative to the IC_{50} value for wild-type HIV-$1_{ERS104pre}$. All assays were conducted in duplicate, and the data shown represent mean values ± SD derived from the results of two or three independent experiments.

The X-ray crystal structure of wild-type HIV-1 protease co-crystallized with GRL-0519A was refined at the near-atomic resolution of 1.27 Å (PDB ID: 3OK9). The structure comprises the protease dimer and the inhibitor in two orientations related by a 180° rotation with 55/45% occupancies. The protease dimer structure is essentially identical to that in the protease–DRV complex[31] with an RMSD of 0.16 Å on Cα atoms. The inhibitor is bound in the active site cavity through a series of hydrogen bond interactions and weaker CH···O interactions with the main-chain atoms of the HIV-1 protease (Figure 3A). The

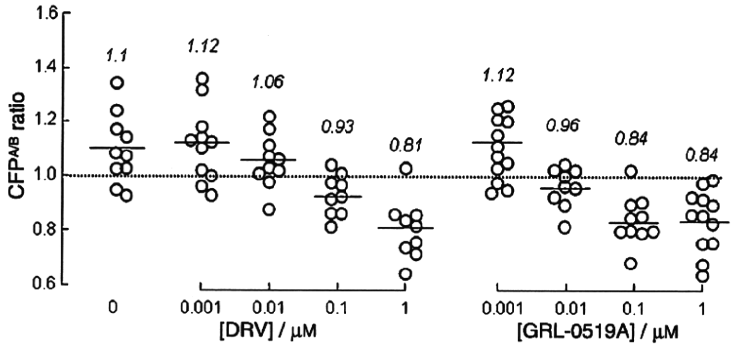

Figure 2. Inhibition of HIV-1 protease dimerization by GRL-0519A. Changes in emission intensity ratios in the presence of DRV or GRL-0519A are shown. COS7 cells were co-transfected with a pair of HIV-PR^{CFP} and HIV-PR^{YFP}, and CFP$^{A/B}$ ratios were determined. The mean values of the ratios are shown as horizontal bars. The results of statistical evaluation of the changes in the CFP$^{A/B}$ ratios determined in the presence or absence of DRV or GRL-0519A are as follows: the CFP$^{A/B}$ ratios in the absence of drug (CFP$^{A/B}_{No\,Drug}$) vs. the CFP$^{A/B}$ ratios in the presence of 0.001 μM DRV (CFP$^{A/B}_{0.001\,DRV}$), $p=0.94$; CFP$^{A/B}_{No\,Drug}$ vs. CFP$^{A/B}_{0.01\,DRV}$, $p=0.15$; CFP$^{A/B}_{No\,Drug}$ vs. CFP$^{A/B}_{0.1\,DRV}$, $p=0.0042$; CFP$^{A/B}_{No\,Drug}$ vs. CFP$^{A/B}_{1.0\,DRV}$, $p=0.0004$; CFP$^{A/B}_{No\,Drug}$ vs. CFP$^{A/B}_{0.001\,GRL\text{-}519}$, $p=0.947$; CFP$^{A/B}_{No\,Drug}$ vs. CFP$^{A/B}_{0.01\,GRL\text{-}519}$, $p=0.0077$; CFP$^{A/B}_{No\,Drug}$ vs. CFP$^{A/B}_{0.1\,GRL\text{-}519}$, $p=0.0003$; CFP$^{A/B}_{No\,Drug}$ vs. CFP$^{A/B}_{1.0\,GRL\text{-}519}$, $p=0.0002$; CFP$^{A/B}_{0.01\,DRV}$ vs. CFP$^{A/B}_{0.01\,GRL\text{-}519}$, $p=0.013$. Panel A: HIV$_{WT}$ vs. rHIV$_{WTpro}^{75/219gag}$, $p=0.53$; HIV$_{WT}$ vs. rHIV$_{WTpro}^{12/75/219/309/409gag}$, $p=0.0080$; HIV$_{WT}$ vs. rHIV$_{WTpro}^{219/409gag}$, $p=0.22$; rHIV$_{WTpro}^{75/219gag}$ vs. rHIV$_{WTpro}^{12/75/219/309/409gag}$, $p=0.0065$; rHIV$_{WTpro}^{75/219gag}$ vs. rHIV$_{WTpro}^{219/409gag}$, $p=0.15$; rHIV$_{WTpro}^{12/75/219/309/409gag}$ vs. rHIV$_{WTpro}^{219/409gag}$, $p=0.0018$. Panel B: HIV$_{WT}$ vs. rHIV$_{WTpro}^{75/219gag}$, $p=0.65$; HIV$_{WT}$ vs. rHIV$_{WTpro}^{12/75/219/309/409gag}$, $p<0.0001$; HIV$_{WT}$ vs. rHIV$_{WTpro}^{219/409gag}$, $p<0.0001$.

major conformation of the inhibitor forms hydrogen bonding interactions of its urethane NH group with the carbonyl oxygen of Gly27. The oxymethyl oxygen of the *tris*-THF interacts with the amide of Asp30, and the second THF oxygen forms hydrogen bonds with the amides of Asp29, Asp30, and the carboxylate side chain of Asp30. In addition, water-mediated interactions connect the inhibitor carbonyl oxygen and sulfonamide oxygen with the amides of Ile50 and 50′ in the flaps, and link the inhibitor P2′ aromatic ring with the amide of Asp30′. Similar interactions are shared by the protease–DRV complex, and are considered responsible for the high affinity of DRV for HIV protease and its potency against drug-resistant HIV-1 variants.[31]

The majority of differences are confined in the interactions of the third THF moiety in GRL-0519A. The third THF ring forms CH···O interactions with Gly48 in the protease flap and water-mediated hydrogen bonds with conserved residues at the dimer interface as shown in Figure 3B. The third THF ring forms CH···O and water-mediated interactions with the carbonyl and amide of Gly48 that may stabilize the flexible flap conformation. The oxygen at the opposite side of the THF ring forms a hydrogen bond with a conserved water molecule and stabilizes a network of hydrogen bonds and ionic interactions connecting Arg8′ from the other subunit with the side chains of Asp29 and Arg87, as well as with the main-chain carbonyl oxygen atoms of Thr26 and Gly27 in the characteristic catalytic triplet (Asp25-Thr26-Gly27) of aspartic proteases. The ionic and hydrogen bonding interactions of Arg8′ with Asp29 and Arg87 are conserved among HIV protease structures and are important components of the dimer interface.[32,33] Also, the oxygen of the third THF ring interacts with a semicircular network of three conserved water molecules that surround the guanidine side chain of Arg8′. The hydrogen bond and van der Waals interactions of the third THF restrain the Arg8′ side chain in a single conformation, thus preventing the formation of an alternate conformation observed in the DRV complex. Furthermore, the third THF ring packs neatly against the P1 phenyl group of the inhibitor with better internal hydrophobic contacts than are possible for *bis*-THF in DRV. The ring stereochemistry (*SSS*-type) in the *tris*-THF ligand of **3** would not be able to make similar hydrophobic contacts. Thus, the *tris*-THF ring of GRL-0519A (**4**) fills the substrate binding cavity better than the *bis*-THF ligand of DRV, anchors Arg87 at the dimer interface, and forms new CH···O and conserved water-mediated interactions with the flaps and the base of the substrate binding cavity.

In conclusion, we designed and synthesized novel oxatricyclic [3(*R*), 3a*S*, 4a*S*, 6a*R*, 7a*S*] and [3(*R*), 3a*S*, 4a*R*, 6a*S*, 7a*S*] ligands and incorporated these ligands in the (*R*)-hydroxyethyl sulfonamide isostere.[16] The orientation, ring size, and stereochemistry are all critical to the potency of the oxatricyclic ligand-derived inhibitors. The ligands were synthesized with defined stereochemistry in optically active forms. Incorporation of a *syn-syn-syn*-fused *tris*-THF led to inhibitor **3**, which has significantly decreased enzyme inhibitory and antiviral potency relative to DRV. However, the *tris*-THF ligand with a *syn-anti-syn* fusion provided inhibitor GRL-0519A (**4**), which has remarkable enzyme inhibitory and antiviral activity. Of particular interest, GRL-0519A displayed potent activity against a variety of multidrug-resistant clinical HIV-1 strains, with EC_{50} values ranging from 0.6 to 4.3 nM, a nearly 10-fold improvement over darunavir. Moreover, GRL-0519A blocked protease dimerization at least 10-fold more potently than DRV. An X-ray crystal structure of GRL-0519A-bound HIV-1 protease revealed molecular insight into the ligand–binding site interactions responsible for its potency against wild-type and mutant viruses. It appears that the first and second THF rings of the *tris*-THF ligand with a *syn-anti-syn* configuration maintain key backbone hydrogen bonding interactions similar to the *bis*-THF ligand of darunavir. The third THF ring oxygen makes water-mediated hydrogen bonds with Asp29, Arg8′, and Gly27. In addition, the ring fills the hydrophobic pocket in the S2 subsite and also stacks nicely behind the P1 phenylmethyl substituent at the S1 subsite. Therefore, our basic design strategy has shown to be extremely powerful and is well worth further experimentation.

Acknowledgements

This research was supported by grants from the National Institutes of Health (GM53386, A.K.G. and GM62920, I.W.). This work was also supported by the Intramural Research Program of the Center for Cancer Research, National Cancer Institute, National Institutes of Health and in part by a Grant-in-aid for Scientific Research (Priority Areas) from the Ministry of Education, Culture,

